

# Dynamic effective stress analysis using the finite element approach

for soils and soil-structure interactions

By Dr. Guoxi Wu  
BC Hydro / Wutec Geotechnical Int.

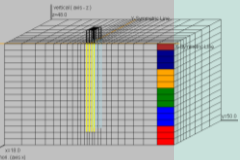
March 2017, 2018, 2019, 2020, 2021, 2022

February 15 & March 15, 2023

Download VERSAT-2D\_Open from:

**VERSAT-2D v.2019.10** *(new)* - *OPEN standalone version (max. 1500 elements) free for everyone*

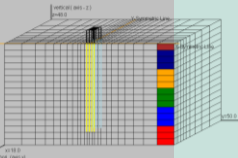
A laptop with Windows OS is needed for this class



# Dynamic effective stress analysis using the finite element approach by Dr. G. Wu

## Lecture Outlines for CIVL581:

1. Finite element dynamic analysis – linear elastic (*30 min*)
  - Finite element formulations
  - Constant stiffness/modulus
  - Dynamic analysis equations; Viscous damping only
2. Nonlinear finite element analysis (*20 min*)
  - Strain-dependent soil stiffness, i.e., soil modulus
  - Strain-dependent soil damping, i.e., hysteretic damping
3. VERSAT-1D site response analysis of soil column for 30m/100m/200m (*45 min*)
4. Effective stress analysis – dynamic pore water pressures (*20 min*)
  - Pore water pressure (PWP) models
  - Stiffness softening; Soil liquefaction and residual strengths
  - Large ground deformations and failures
5. Analysis of Upper San Fernando Dam – Case History Study (*60 min*)
6. Other Case Analyses (*10 min*)



### 1. Finite element dynamic analysis: linear elastic (2D plane strain, $\varepsilon_z=0$ )

- 1.1 Finite element formulations:**

A continuous cross section is divided into many small areas (elements), no overlapping, no gaps/voids (except tunnels, or holes). In an element, nodes are always located on the boundaries (not within), and nodes are numbered counterclockwise. - **3 governing equations ( $\sigma - \varepsilon$ ,  $\varepsilon - \delta$ , and force equilibrium)**

[1] STRESS – STRAIN Relationship (B=bulk modulus; G=shear modulus):

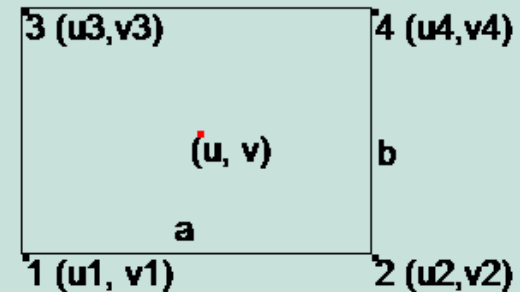
$$\begin{Bmatrix} \sigma_x \\ \sigma_y \\ \tau_{xy} \end{Bmatrix} = \begin{bmatrix} B + 4G/3 & B - 2G/3 & 0 \\ B - 2/3G & B + 4G/3 & 0 \\ 0 & 0 & G \end{bmatrix} \begin{Bmatrix} \varepsilon_x \\ \varepsilon_y \\ \gamma_{xy} \end{Bmatrix} = [D] \{\varepsilon\}$$

[2a] Relationship between Displacements  $\begin{Bmatrix} u \\ v \end{Bmatrix}$  and Node Displacements  $\{\delta\} = \begin{Bmatrix} u_i \\ v_i \end{Bmatrix}$  is defined by shape functions (geometry):  $N_i(x,y)$  with  $i=1$  to 4 (see figure below)

$$\begin{Bmatrix} u \\ v \end{Bmatrix} = \sum_1^4 N_i(x,y) \begin{Bmatrix} u_i \\ v_i \end{Bmatrix} \quad \text{for 4-node element shown}$$

For a rectangular element with node 1 at (0,0) and two side length of a and b, then:

$$\begin{aligned} N_1(x,y) &= \left(1 - \frac{x}{a}\right) \left(1 - \frac{y}{b}\right); & N_2(x,y) &= \frac{x}{a} \left(1 - \frac{y}{b}\right); \\ N_3(x,y) &= \left(1 - \frac{x}{a}\right) \frac{y}{b}; & N_4(x,y) &= \frac{x}{a} \frac{y}{b}; \end{aligned}$$



### 1. Finite element dynamic analysis – linear elastic (2D plane strain)

- **1.1 Finite element formulations:**

[2b] STRAIN – DISPLACEMENT Relationship:

$$\begin{Bmatrix} \varepsilon_x \\ \varepsilon_y \\ \gamma_{xy} \end{Bmatrix} = \begin{Bmatrix} \frac{\partial u}{\partial x} \\ \frac{\partial v}{\partial y} \\ \frac{\partial u}{\partial y} + \frac{\partial v}{\partial x} \end{Bmatrix} = [B^*] \{\delta\}$$

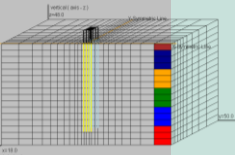
$$\begin{bmatrix} \frac{\partial N_1(x,y)}{\partial x} & 0 & \frac{\partial N_2(x,y)}{\partial x} & 0 & \frac{\partial N_3(x,y)}{\partial x} & 0 \\ 0 & \frac{\partial N_1(x,y)}{\partial y} & 0 & \frac{\partial N_2(x,y)}{\partial y} & 0 & \frac{\partial N_3(x,y)}{\partial y} \\ \frac{\partial N_1(x,y)}{\partial y} & \frac{\partial N_1(x,y)}{\partial x} & \frac{\partial N_2(x,y)}{\partial y} & \frac{\partial N_2(x,y)}{\partial x} & \frac{\partial N_3(x,y)}{\partial y} & \frac{\partial N_3(x,y)}{\partial x} \end{bmatrix} \begin{Bmatrix} u_1 \\ v_1 \\ \vdots \end{Bmatrix}$$

[3] Virtual work theory to derive Force (external) – Stress (internal) equilibrium:

$$\{\delta\}^T \{F\} = \iint \varepsilon^T \sigma \, dx dy = \{\delta\}^T \iint [B^*]^T \sigma \, dx dy; \text{ therefore}$$

$$\{F\} = \iint [B^*]^T \sigma \, dx dy \quad ; \text{ and, therefore}$$

$$\{F\} = \iint [B^*]^T [D] [B^*] \, dx dy \cdot \{\delta\}$$



### 1. Finite element dynamic analysis – linear elastic (2D plane strain)

- **1.1 Finite element formulations: static loading only**

$$[K] \{\delta\} = \{F\}$$

Where the Stiffness Matrix [K]:

$$[K] = \iint [B^*]^T [D] [B^*] dx dy \quad \text{integral over the element area;}$$

- **1.2 Linear elastic static analysis:**

Matrix equations:  $[K] \{\delta\} = \{F\}$  with boundary conditions

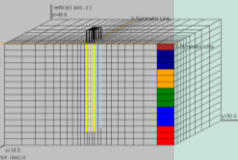
⇒ obtain displacement solutions  $\{\delta\}$  ⇒ obtain strains, then stresses in each element.

- constant modulus G and B.
- constant [D], and
- thus constant stiffness matrix [K]

Derivation of Young's modulus (E) and Poisson's Ratio ( $\mu$ ):

$$E = 2(1 + \mu) \bullet G$$

$$\mu = \frac{3B - 2G}{6B + 2G}$$



- **1.3 Dynamic Analysis Equations** in matrix form:

$$[M] \left\{ \Delta \frac{d^2 \delta}{dt^2} \right\} + [C] \left\{ \Delta \frac{d\delta}{dt} \right\} + [K] \{ \Delta \delta \} = \{ \Delta P \}$$

Where

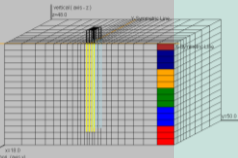
[M]	= mass matrices
[C]	= viscous damping matrices
[K]	= tangent stiffness matrices
[ $\Delta\delta$ ]	= incremental displacement matrices
[ $\Delta d\delta/dt$ ]	= incremental velocity matrices
[ $\Delta d^2\delta/dt^2$ ]	= incremental acceleration matrices
[ $\Delta P$ ]	= incremental external load matrices

- Eigen values and modal angular frequencies:  $\omega_1, \omega_2, \omega_3, \omega_4, \dots$

$$([K] - \omega^2 [M]) = 0$$

frequencies (Hz):  $f_1, f_2, f_3, f_4 = \omega_1/(2\pi), \omega_2/(2\pi), \omega_3/(2\pi), \omega_4/(2\pi), \dots$

structural periods:  $T_1, T_2, T_3, T_4 = (2\pi)/\omega_1, (2\pi)/\omega_2, (2\pi)/\omega_3, (2\pi)/\omega_4, \dots$



- Viscous damping only: In a linear elastic analysis, system damping consists only of viscous damping (inside) and radiation damping (at boundaries). Viscous damping is velocity proportional: typical used 5%

Viscous damping in **VERSAT** program:

Rayleigh type (b: high frequency damping constant; a: low ...constant)

$$[C] = a[M] + b[K]$$

$$a = 2\lambda_m\omega_1$$

$$b = 2\lambda_k/\omega_1 \quad \text{OR: } \lambda_m = \frac{a}{2\omega}$$

$$\text{OR: } \lambda_k = \frac{b\omega}{2}$$

The total damping at the first mode  $\omega_1$  is

$$\lambda = \lambda_k + \lambda_m$$

$\lambda_m$  = the mass proportional Raleigh damping (%) at first mode;

$\lambda_k$  = the stiffness proportional Raleigh damping (%) at first mode.

**Example:** With  $f_1=1.0$  Hz or  $\omega_1 = 6.28$ , 1% mass and 2% stiffness damping, then:

$$a=0.1256$$

$$b=0.0064$$

# Dynamic effective stress analysis using the finite element approach by Dr. G. Wu

## 1. Linear Elastic

### Input ground motions Options in **VERSAT**

- 1) *Within motion*: Acceleration input at the rigid base, incremental inertial forces on the soil mass caused by base accelerations are computed using the Newton's law and applied as  $[\Delta P]$ , i.e.,  $[\Delta P] = [M] \{\Delta \text{base\_acceleration}\}$
- 2) *outcropping motion*: Velocity time history input,  $v_0(t)$ , at the elastic base, incremental shear forces at the base nodes are determined and applied as  $[\Delta P]$

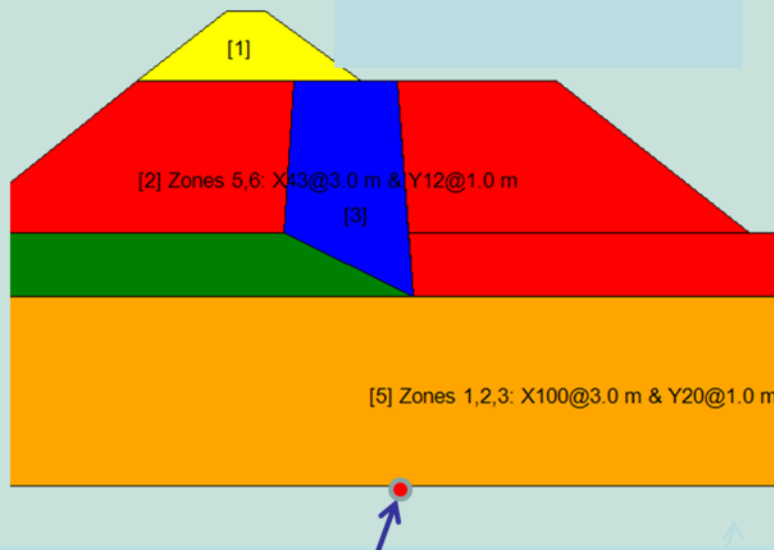


Figure Rigid Base, ground motion is measured within the base

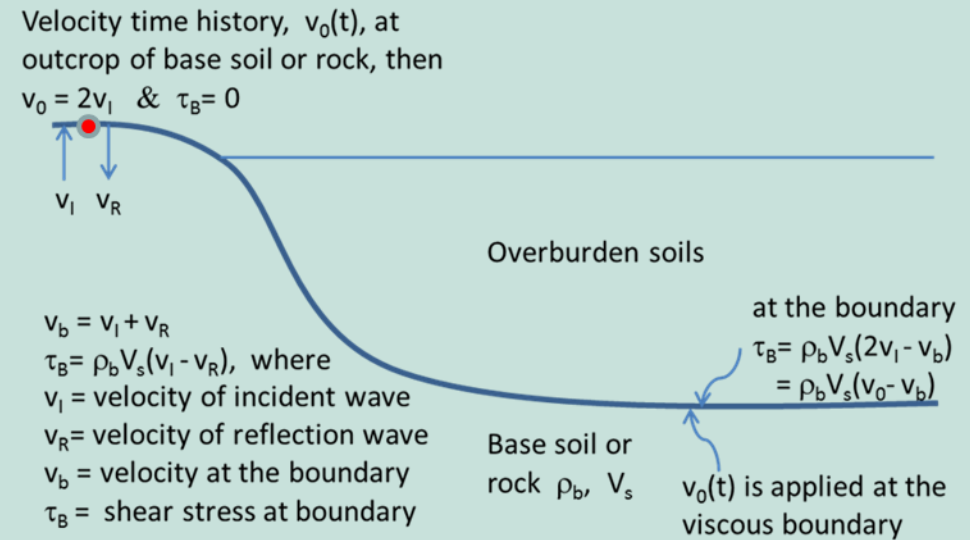
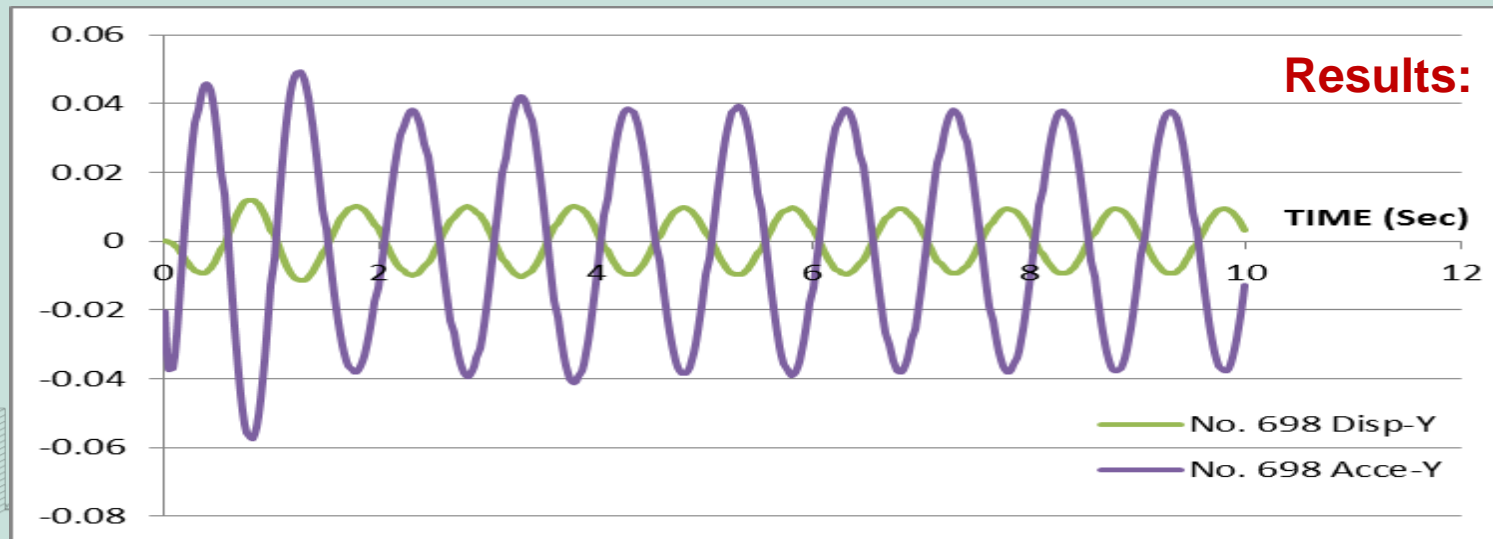
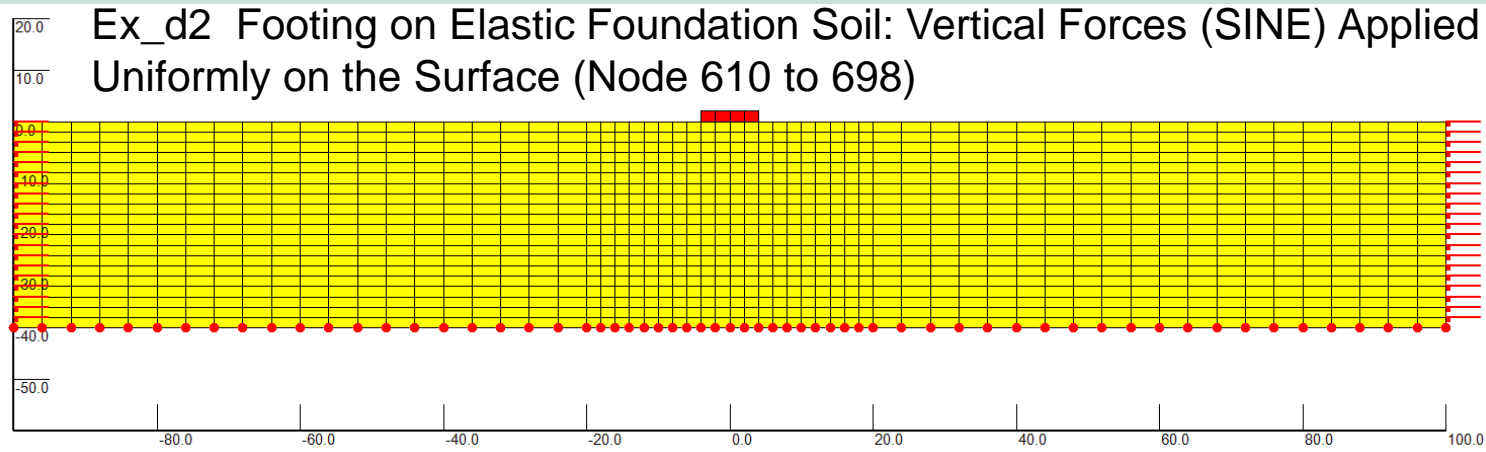


Figure The elastic base model with a viscous boundary

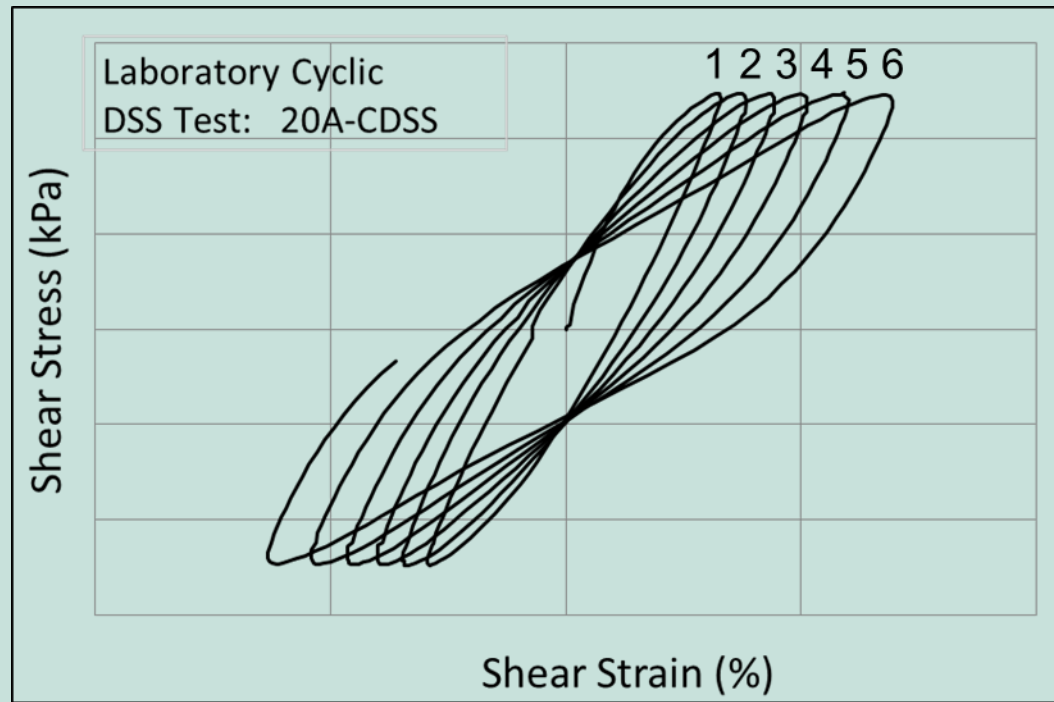
# Dynamic effective stress analysis using the finite element approach by Dr. G. Wu

## 1. Linear Elastic



## 2.0 Non-linear shear stress – strain relationship

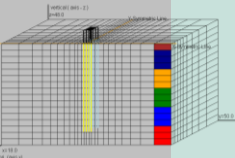
Example stress – strain hysteresis loops for **6 cycles** of constant shear stress from laboratory Cyclic Direct Simple Shear (cyclic DSS):



Observations:

1. In a loop, shear modulus ( $G$ ) decrease with increasing strain level: nonlinear
2. With cycles, the loop area increases, becomes fatter => high damping; i.e., soil material damping increases with increasing strain level;
3. With cycles, the loops become flatter under same stress level: PWP effect.

*Note: Material damping is also called “hysteretic damping”: stress – strain path dependent, not velocity dependent; up to 30%*



**2.1 Shear modulus, G: reduces with increased shear strain, nonlinear**

At low strain (~ 0.001%):  $G_{max} = \rho V_s^2$

$V_s$ : shear wave velocity, normally measured by seismic cross-hole (downhole) survey

An idealized nonlinear model: hyperbolic  $\tau_{xy} - \gamma$  relation

$$\tau_{xy} = \frac{G_{max} \gamma}{1 + G_{max} / \tau_{ult} \bullet |\gamma|}$$

Secant shear modulus:

(in SHAKE frequency domain, equivalent linear analysis)

$$G / G_{max} = \frac{1}{(1 + R_f \bullet |\gamma|)}$$

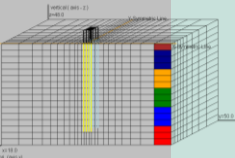
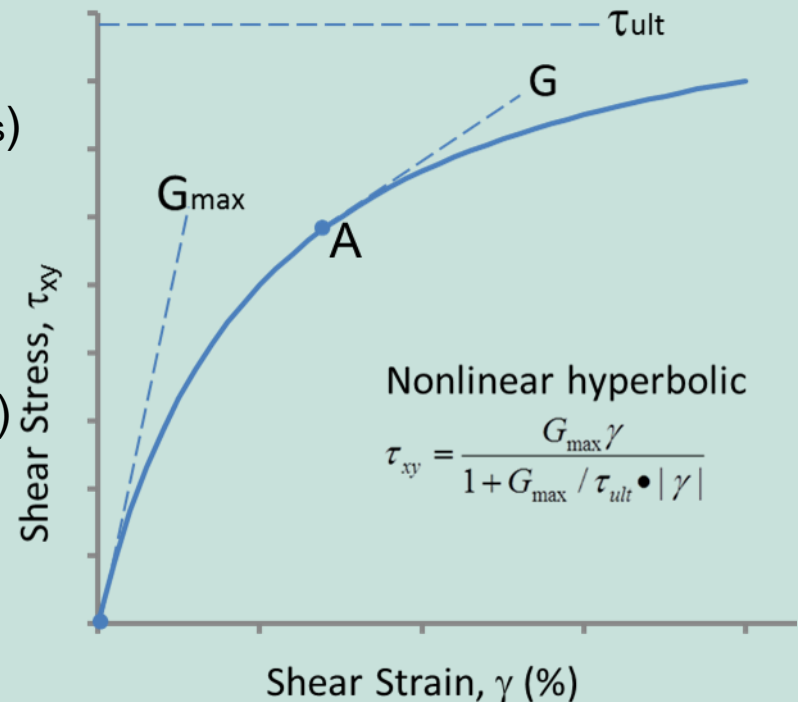
Tangent shear modulus:

(in TARA-3, VERSAT-2D time domain nonlinear analysis)

$$G / G_{max} = \frac{1}{(1 + R_f \bullet |\gamma|)^2}$$

Where modulus reduction factor:

$$R_f = \frac{G_{max}}{\tau_{ult}}$$

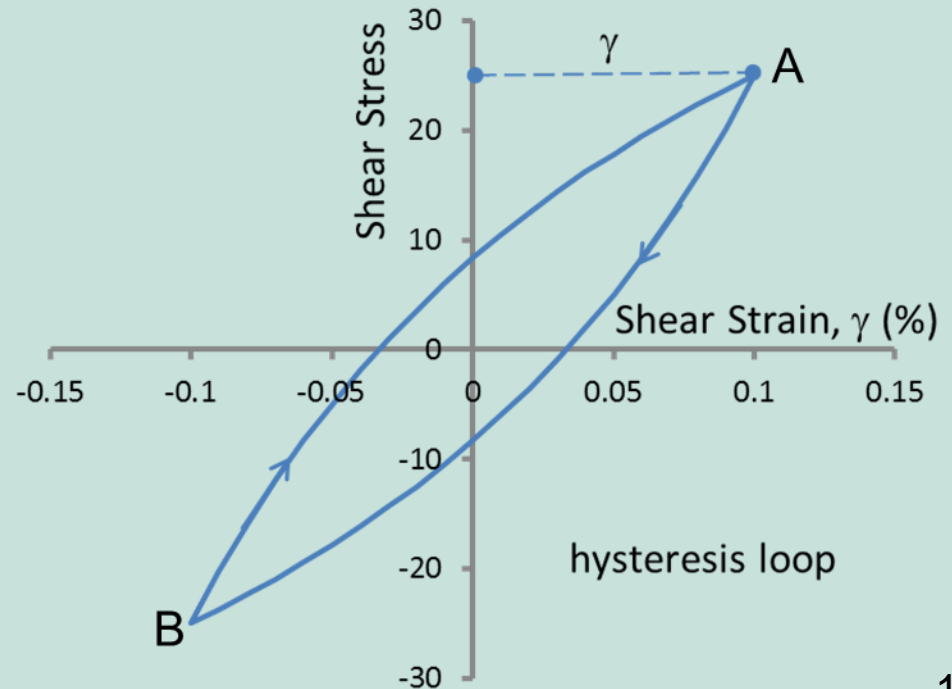
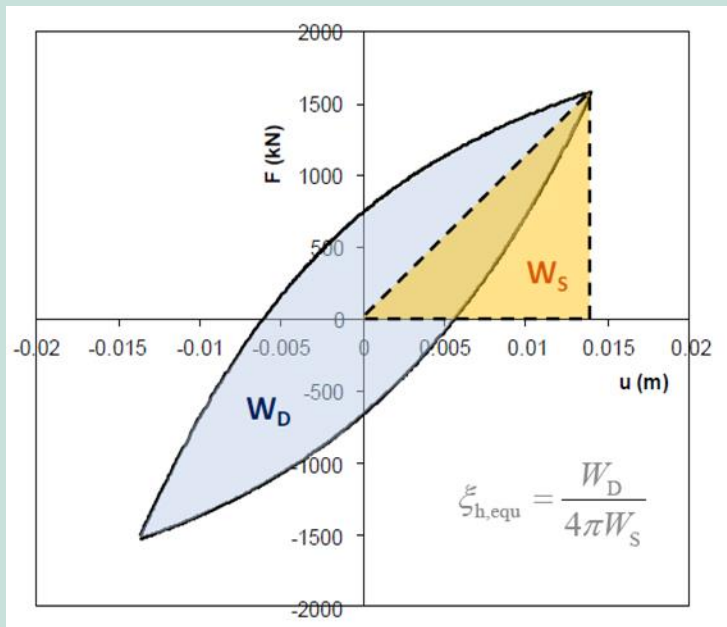


## 2.2 Material damping: implied in a hysteresis loop

Hysteretic damping ratio from a hyperbolic  $\gamma - \tau$  curve (point A); and apply the Masing-rule on a full **unloading** (from A to B) – **reloading** (from B to A) loop:

$$\lambda = \frac{1}{4\pi} \frac{W_D}{W_S} = \frac{4}{\pi} \left( 1 + \frac{1}{R_f \gamma} \right) \left[ 1 - \frac{1}{R_f \gamma} \ln(1 + \gamma R_f) \right] - \frac{2}{\pi}$$

$$R_f = \frac{G_{max}}{\tau_{ult}}$$



# Dynamic effective stress analysis using the finite element approach by Dr. G. Wu

## 2. Non-Linear

### 2.3 shear modulus and damping: comparison with laboratory data

#### [1] shear modulus reduction with strain (%)

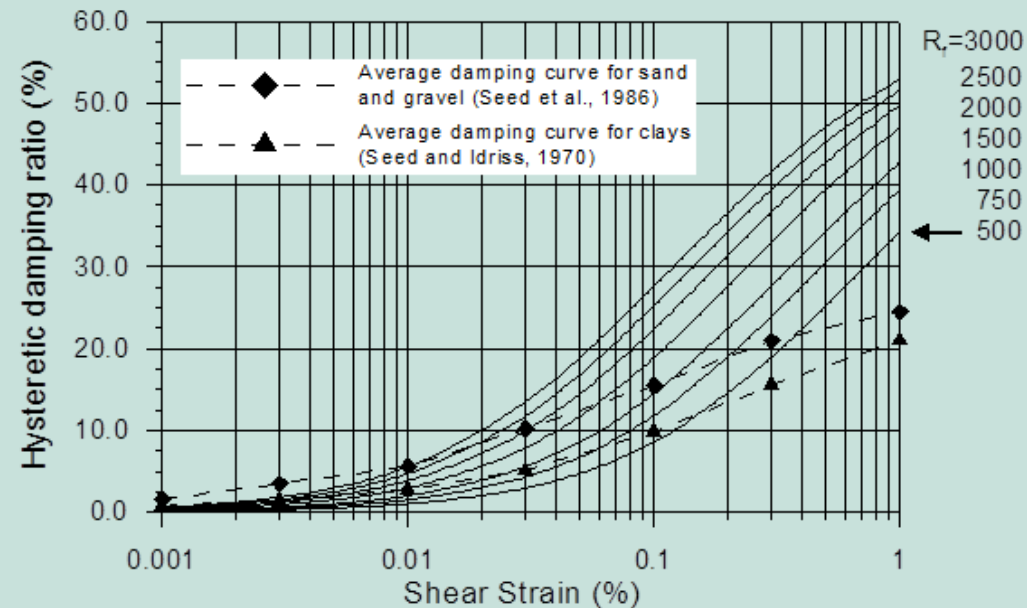
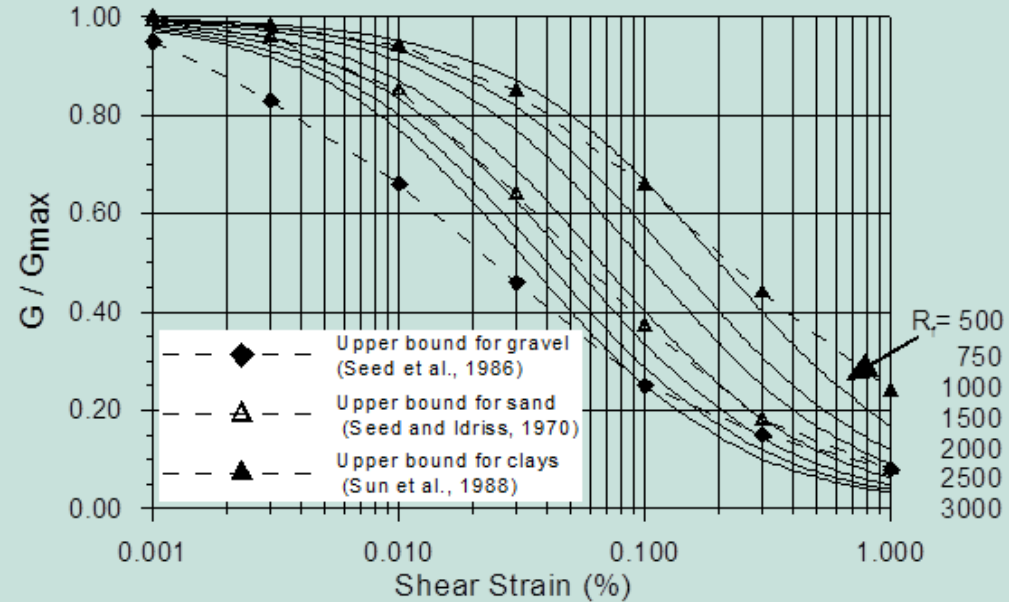
- Most in gravels (75% at 0.1%)
- 2<sup>nd</sup> in sands (60% at 0.1% strain)
- Least in clays (35% at 0.1% strain)

#### [2] soil damping increase with strain

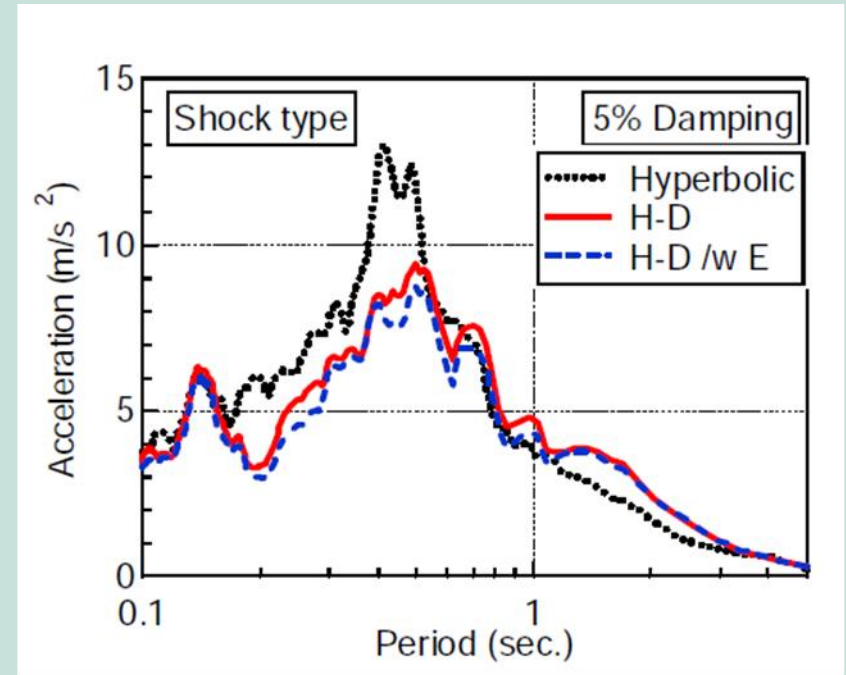
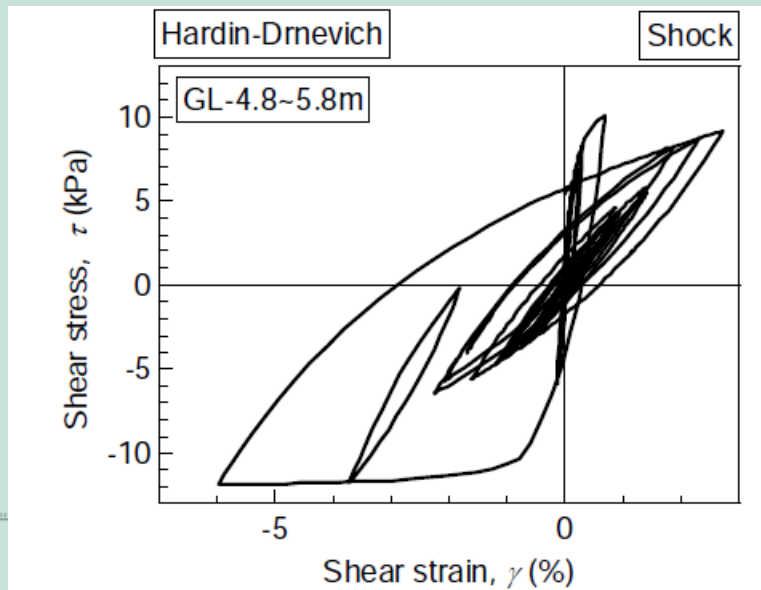
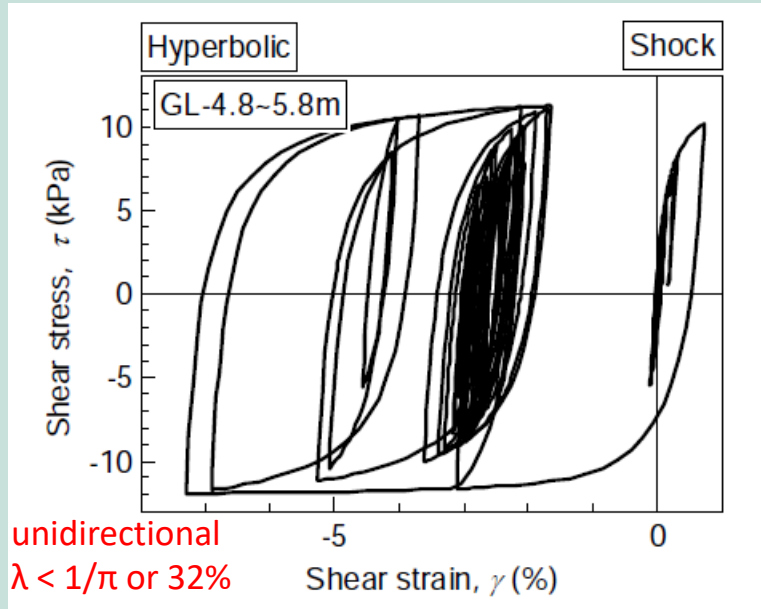
- sands (16% at 0.1% strain)
- clays (10% damping at 0.1% strain)

Note: Wu (2001) for  $R_f$  defined in hyperbolic model

[3] Charts applicable to a full unloading-reloading loop with shear strain extending to both + and - directions. A unidirectional loop has much smaller damping ( $\frac{1}{4}$  to  $\frac{1}{2}$  of what is shown).



- 2.4 Example 1:  
A 16-m soil layer subjected to shock wave at base:  
hyperbolic vs Hardin – Drnevich (H-D) Equation:



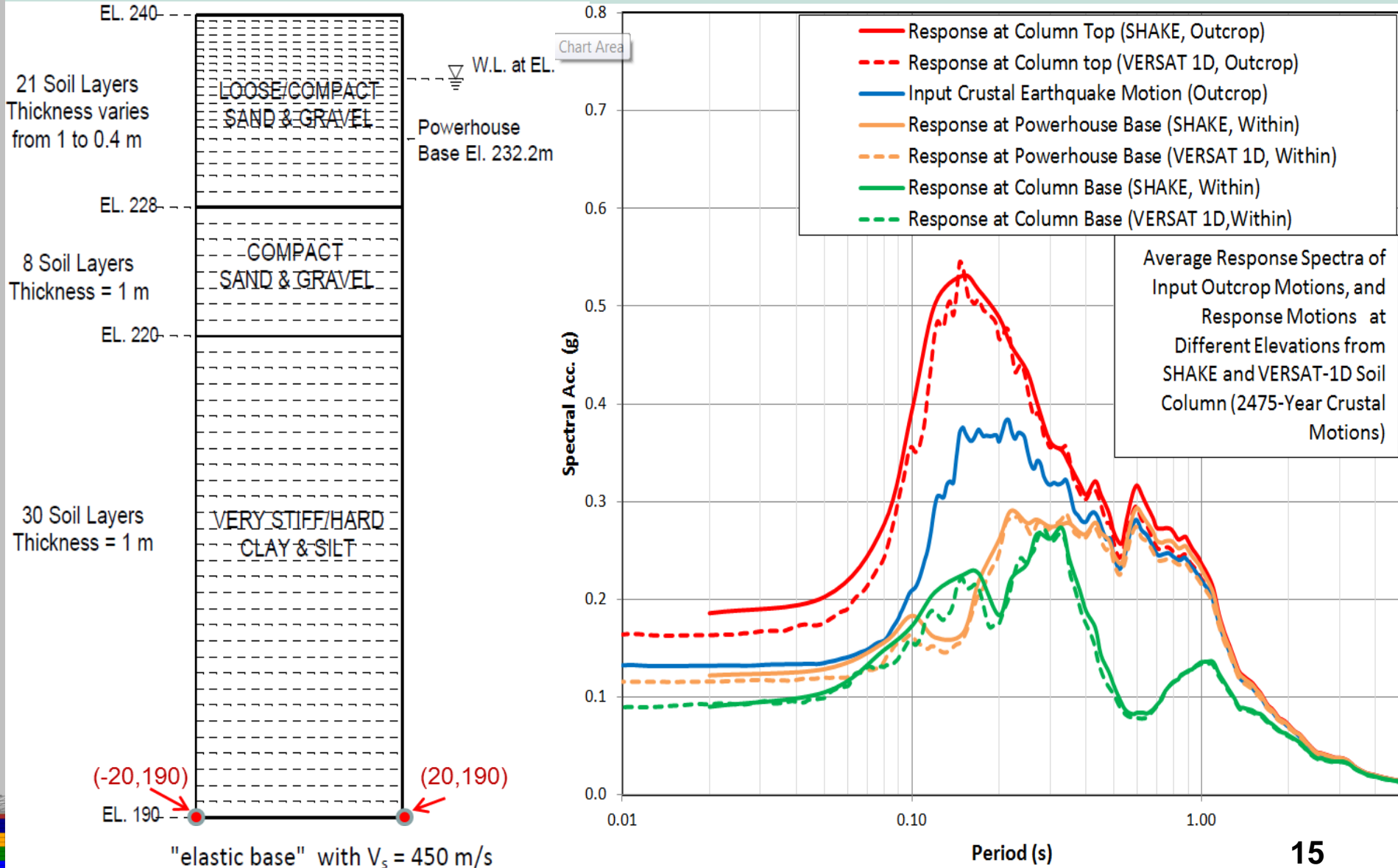
Response spectra from the acceleration at the ground surface

Source: Role of hysteretic damping in earthquake response of ground, N. Yoshida, *Tohoku Gakuin University, Japan, 2011*

# Dynamic effective stress analysis using the finite element approach by Dr. G. Wu

## 2. Non-Linear

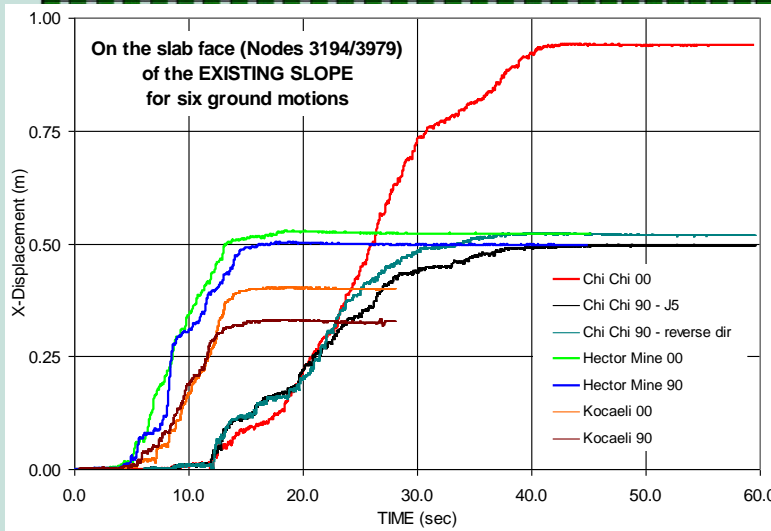
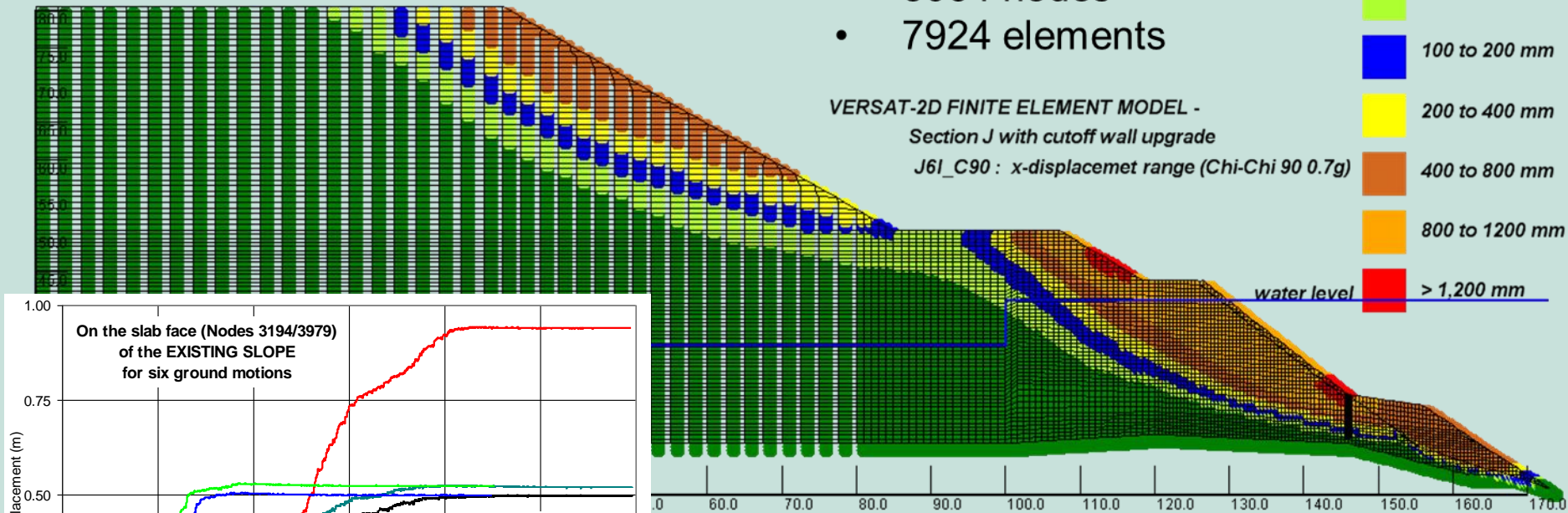
- 2.4 Example 2: Comparison between SHAKE and VERSAT-1D at low-moderate level of earthquake shaking: *SHAKE equivalent linear approximation is able to produce very good representation of true soil nonlinear hysteresis behavior*



- 2.4 Example 3:  
Seismic Upgrade of BC Hydro Ruskin Dam:

- 8064 nodes
- 7924 elements

VERSAT-2D FINITE ELEMENT MODEL -  
Section J with cutoff wall upgrade  
J6I\_C90 : x-displacemet range (Chi-Chi 90 0.7g)

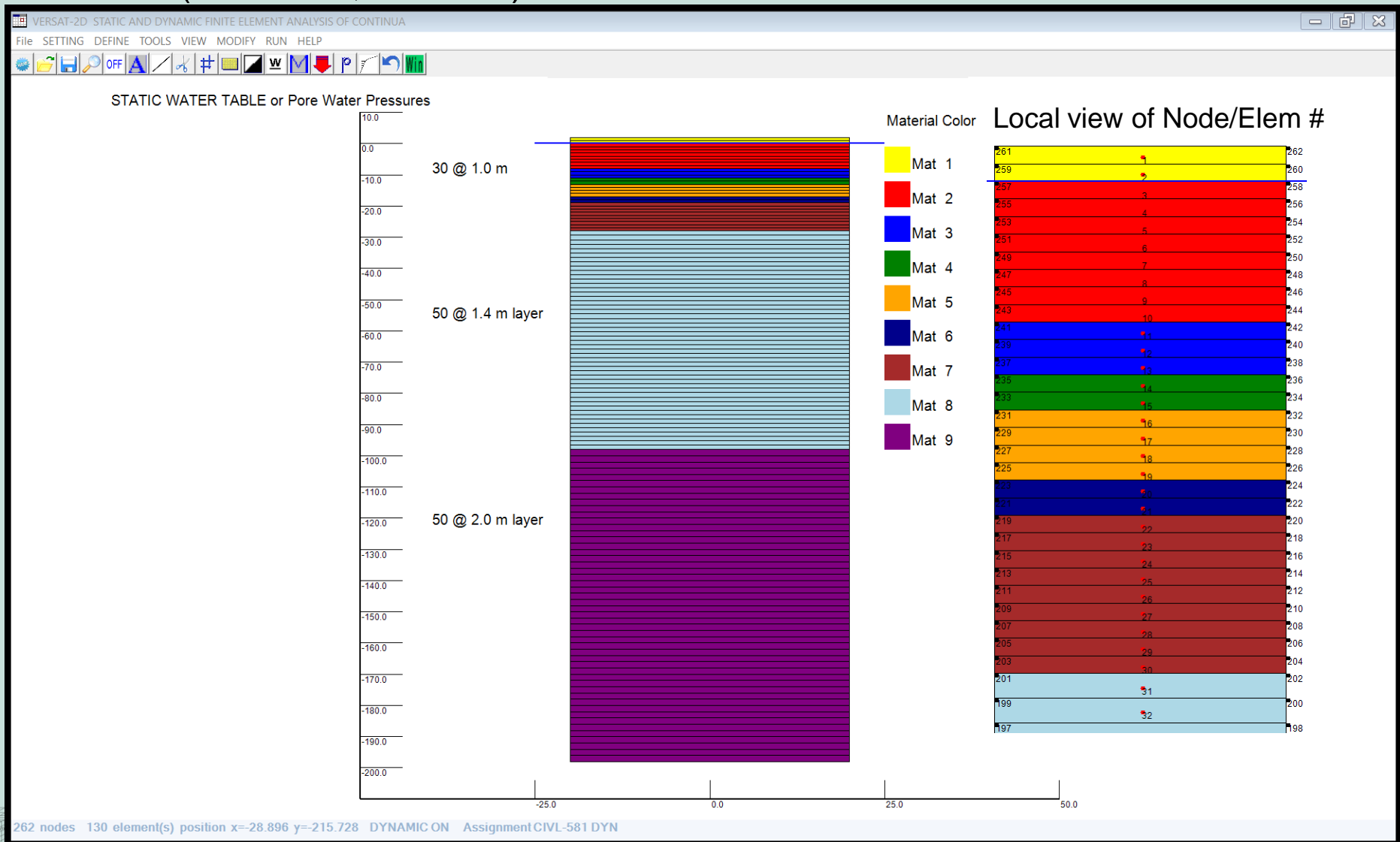


Sweeney, N. and Yan L. 2014. DAM SAFETY UPGRADE OF THE RUSKIN DAM RIGHT ABUTMENT, Canadian Dam Association 2014 Annual Conference, Alberta, Canada

# Dynamic effective stress analysis using the finite element approach by Dr. G. Wu

## 3. 1D Site Response

- 2.4 Assignment #5:  
VERSAT-1D nonlinear site response analysis of a soil column  
200-m (or 100-m, or 30-m)



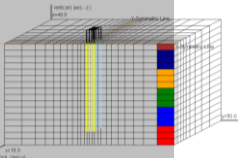
## END OF TODAY'S LECTURE

**Next class will be on 12 pm March 15, 2023**

To prepare:

1. Work on Assignment # 5 – [due March 29, 2023.](#)
2. Download Analysis Example for Upper San Fernando Dam:  
(with PowerPoint Slides on Model Setup and Results)

[http://www.wutecgeo.com/documents/UpperSanFernandoDam\\_Ex\\_d2017.zip](http://www.wutecgeo.com/documents/UpperSanFernandoDam_Ex_d2017.zip)



### 3. Non-linear effective stress analysis:

#### - PWP and liquefaction

“Sand liquefaction is a **fluidization** process of saturated sand mass subject to cycles of shear stress. Under shaking, it can be easily observed that loose sands in a dry container will experience volume contraction and settle to a more compact state. In a saturated condition, immediate volume change of the sand would not occur because water in the pore does not drain quickly enough under the rapid earthquake loading. Instead, the potential for **volume change translates into** a quick increase in excess pore water pressure (**PWP**) in the sand mass. Liquefaction occurs when the PWP exceeds a threshold value that the pore water effectively suspends sand particles. Sand boiling to ground surface is a surficial expression of liquefaction of sands in the ground.” *Guoxi Wu 2015. Seismic Design of Dams, Encyclopedia of Earthquake Engineering published by Springer-Verlag Berlin Heidelberg*

#### 3.1 Pore water pressure (PWP) models:

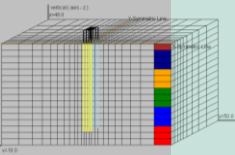
##### [1]. Martin-Finn-Seed model (MFS, 1976)

$$\Delta u = E_r \bullet \Delta \varepsilon_v^p$$
$$\Delta \varepsilon_v^p = C_1 \gamma \bullet \text{Exp}\left(-C_2 \frac{\varepsilon_v^p}{\gamma}\right)$$

$\Delta \varepsilon_v^p$  = Plastic volumetric strain increment accumulated during a period of strain history;

$\Delta u$  = Dynamic pore water pressure increment corresponding to the plastic volumetric strain increment  $\Delta \varepsilon_v^p$

$E_r$  = Rebound modulus of the soil skeleton corresponding to the current effective vertical stress.



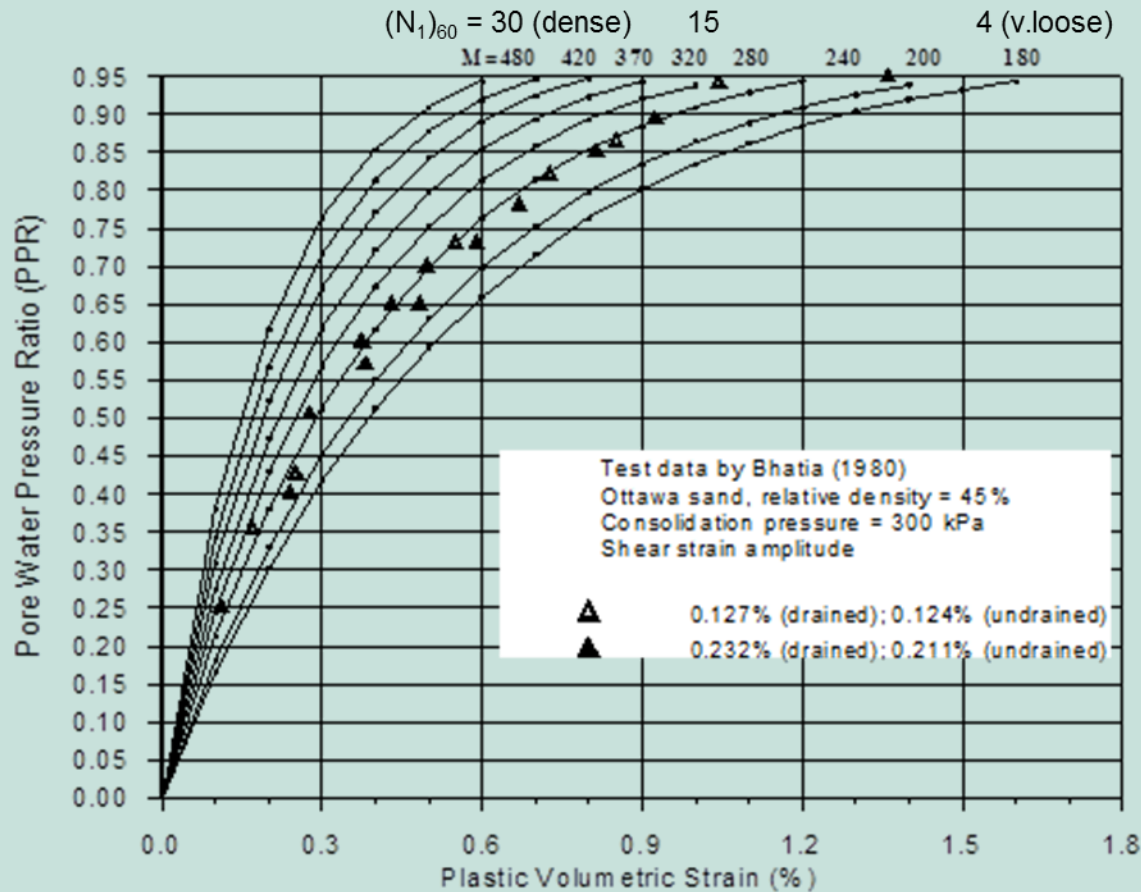
[2] Modified MFS Pore Water Pressure Model (Wu 2001)

$$E_r = M \bullet (\sigma_{v0}' - u)$$

M = rebound modulus constant, increasing with relative density of sands

$\sigma_{v0}'$  = initial effective vertical stress

u = current dynamic pore water pressure



[3]. Seed's Pore Water Pressure Model:

Empirical correlation by Seed et al., 1976

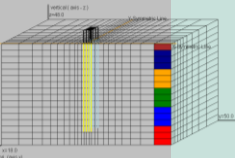
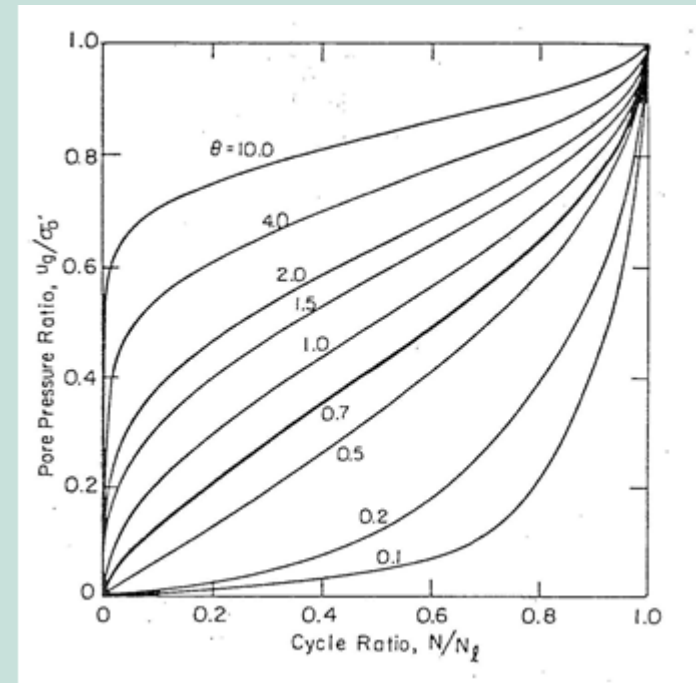
- normalized to liquefaction occurs in 15 cycles

$$u / \sigma_{v0}' = \frac{2}{\pi} \arcsin\left(\frac{N_{15}}{N_l}\right)^{\frac{1}{2\theta}}$$

$\theta$  is an empirical constant;

$N_l$  is the number of uniform shear stress cycles which cause liquefaction, normalized to 15; and

$N_{15}$  is the equivalent number of uniform shear stress cycles.



# Dynamic effective stress analysis using the finite element approach by Dr. G. Wu

## 4. Non-linear Effective stress

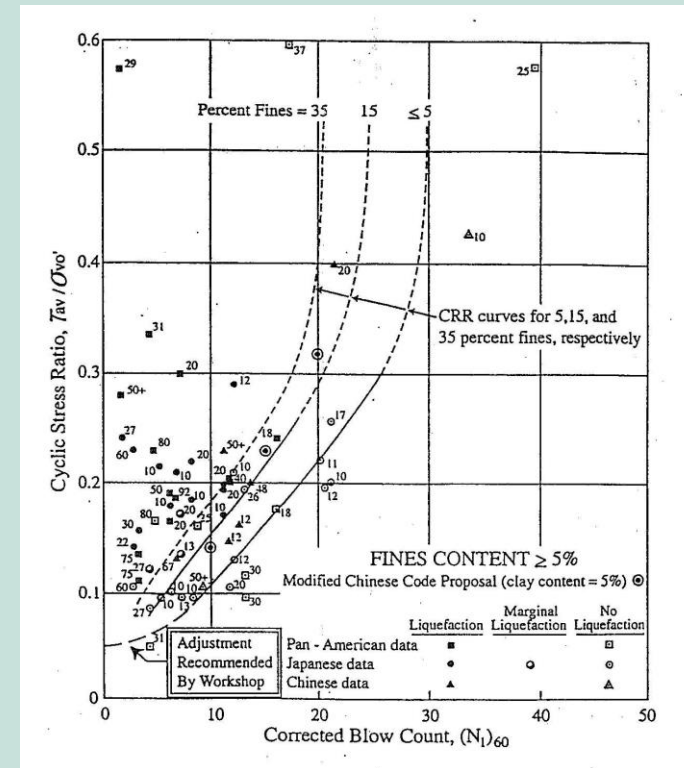
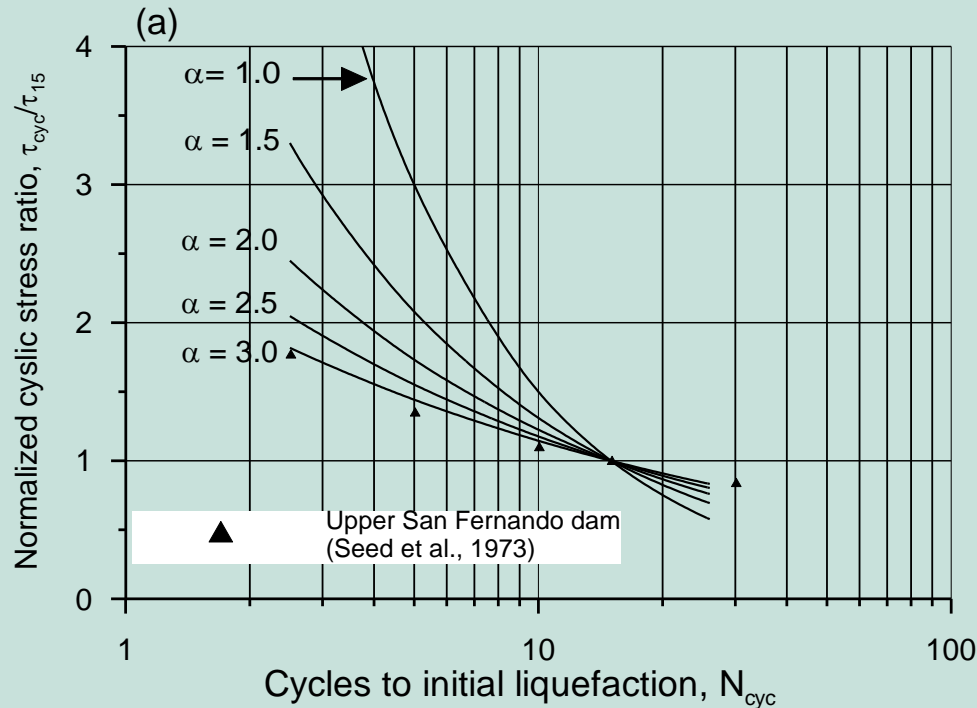
- **3.1 Pore water pressure (PWP) models:**
- [3] Seed's PWP model: calculation of  $N_{15}$

$$N_{15} = \left( \frac{\tau_{cyc}}{\tau_{15}} \right)^\alpha$$

$\alpha$  is a shear stress conversion constant that is directly related to the magnitude scaling factor (MSF) (Wu 2001)

$\tau_{cyc}$  is the shear stress caused by earthquake

$\tau_{15}$  is the shear stress required to cause liquefaction in 15 cycles, can be determined from  $(N_1)_{60}$



# Dynamic effective stress analysis using the finite element approach by Dr. G. Wu

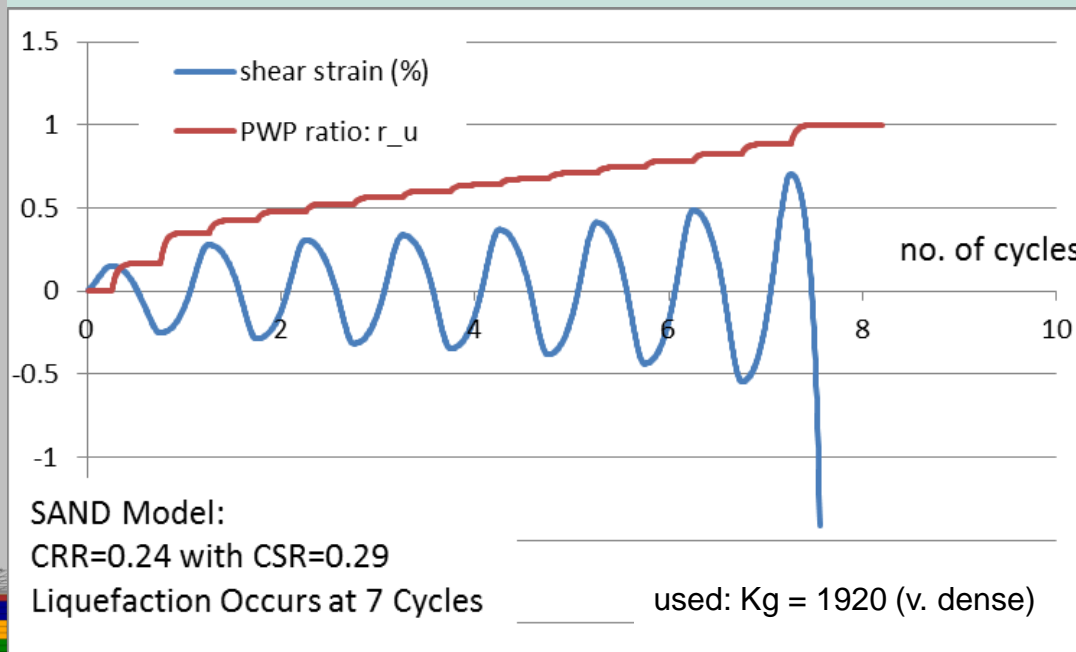
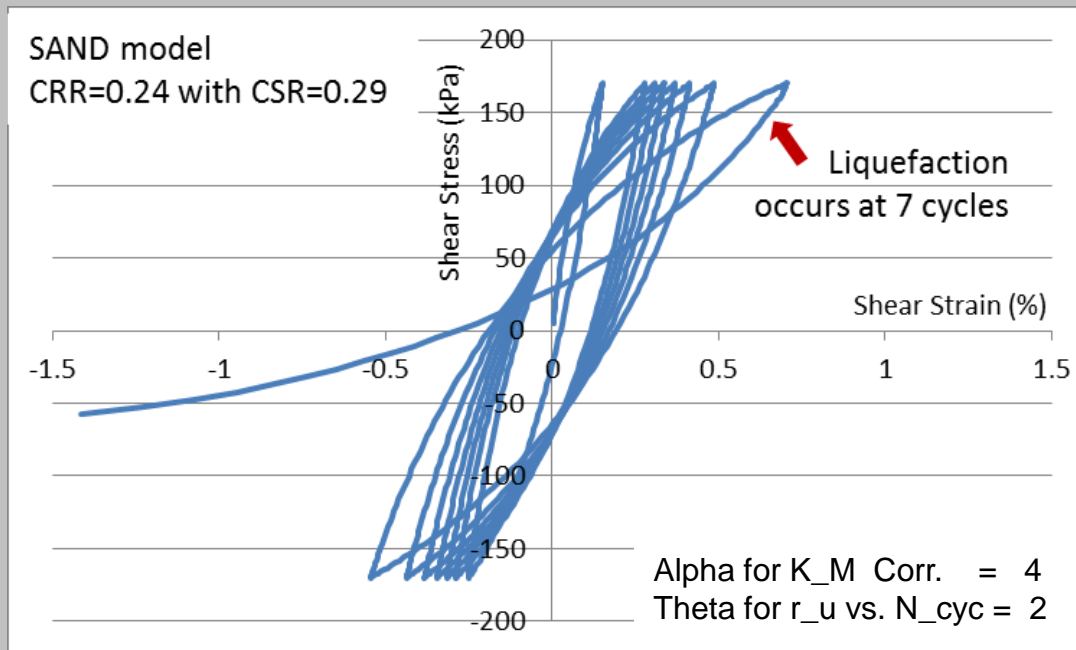
## 4. Non-linear Effective stress

### • 3.2 Liquefaction of Sands:

Liquefaction occurs when the PWP exceeds a threshold value that the pore water effectively suspends sand particles

- PWP ratio ( $r_u$ ) approaches 1.0
- large strains occur
- large deformations occur

Example from a numerical simulation using the “**VERSAT-SAND**” Model



• **3.3 Post Liquefaction Strengths of Sands**

– Residual strengths (Seed, R.B., and Harder, L.F. 1990. SPT-based analysis of cyclic pore pressure generation and undrained residual strength. Proceedings of H. Bolton Seed Memorial Symposium; I. M., and Boulanger, R. W. (2008) “Soil liquefaction during earthquakes”. EERI Monograph MNO-12; and many others)

➤ A key feature of the effective stress analysis is that it allows some elements to liquefy first and others to liquefy at a later time. By doing this, the earlier liquefied soil elements exhibit a softened response that creates an isolation effect for shaking of soil elements above them. The cyclic shear stress history of elements in the upper layers may therefore be significantly affected by the liquefied soil elements below them. - Wu (2001)

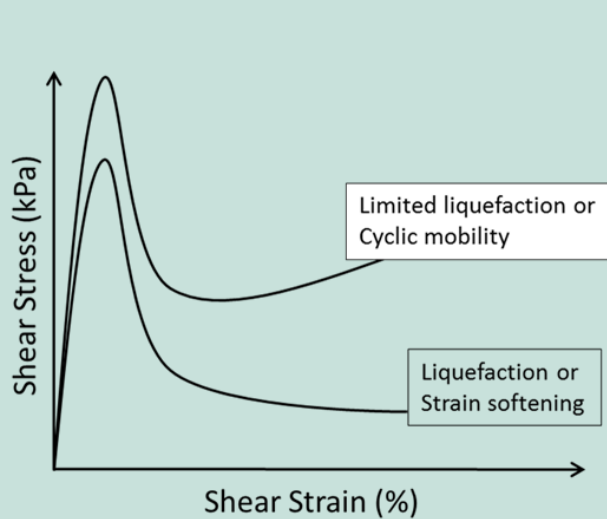


Figure 1 Shear stress – strain response indicating great strength loss after liquefaction and some strength loss with cyclic mobility

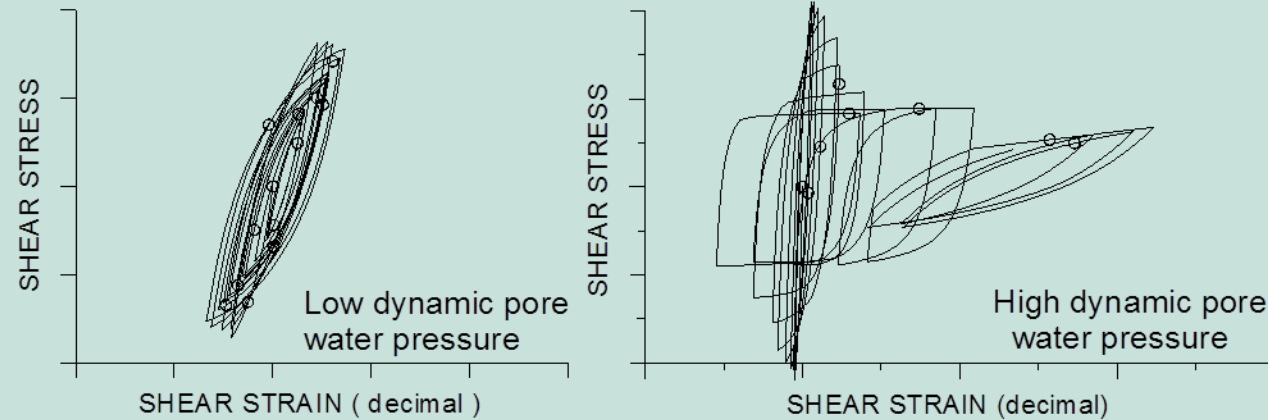
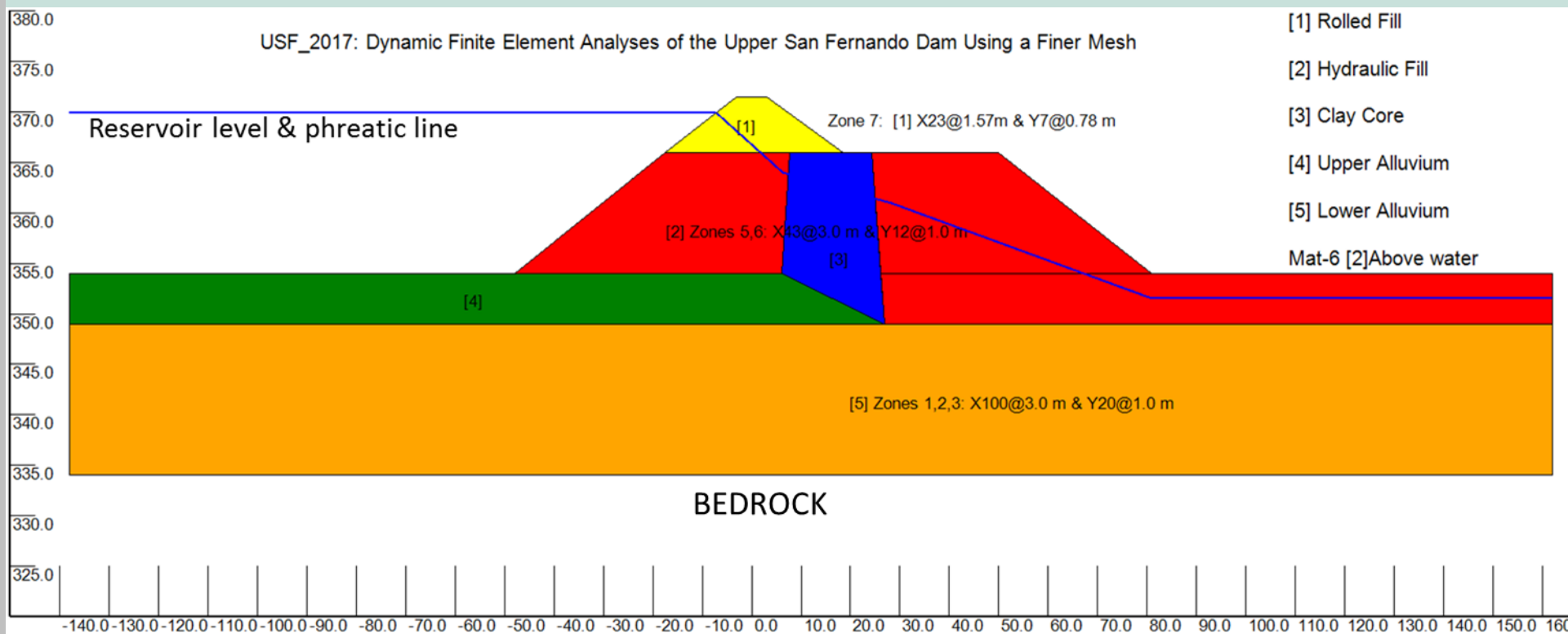


Figure 2 A numerical simulation of pre- and post liquefaction response

- **4.1 Case History Study by Finite Element Approach**  
for Dynamic Analysis Of the Upper San Fernando Dam Under The 1971 San Fernando Earthquake: Pacoima Record (PGA 0.6g) (Wu 2001)

- [1] Model creation:



- **4.1 Case History Study by Finite Element Approach Analysis Of Upper San Fernando Dam Under The 1971 San Fernando Earthquake**
- [1] Model creation:

USF\_2017: Dynamic Finite Element Analyses of the Upper San Fernando Dam Using a Finer Mesh

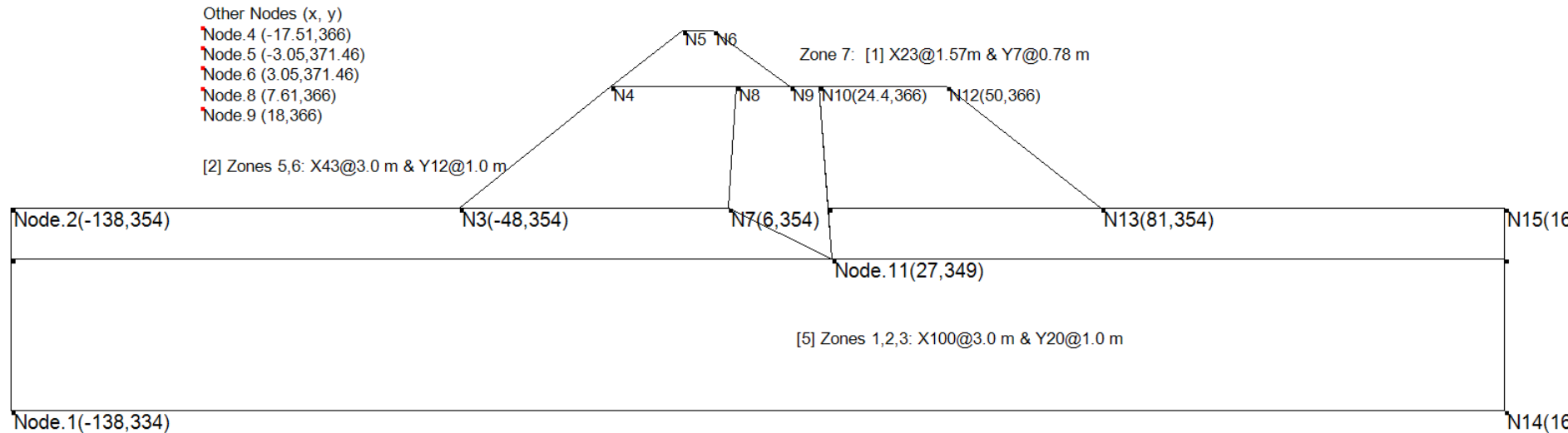
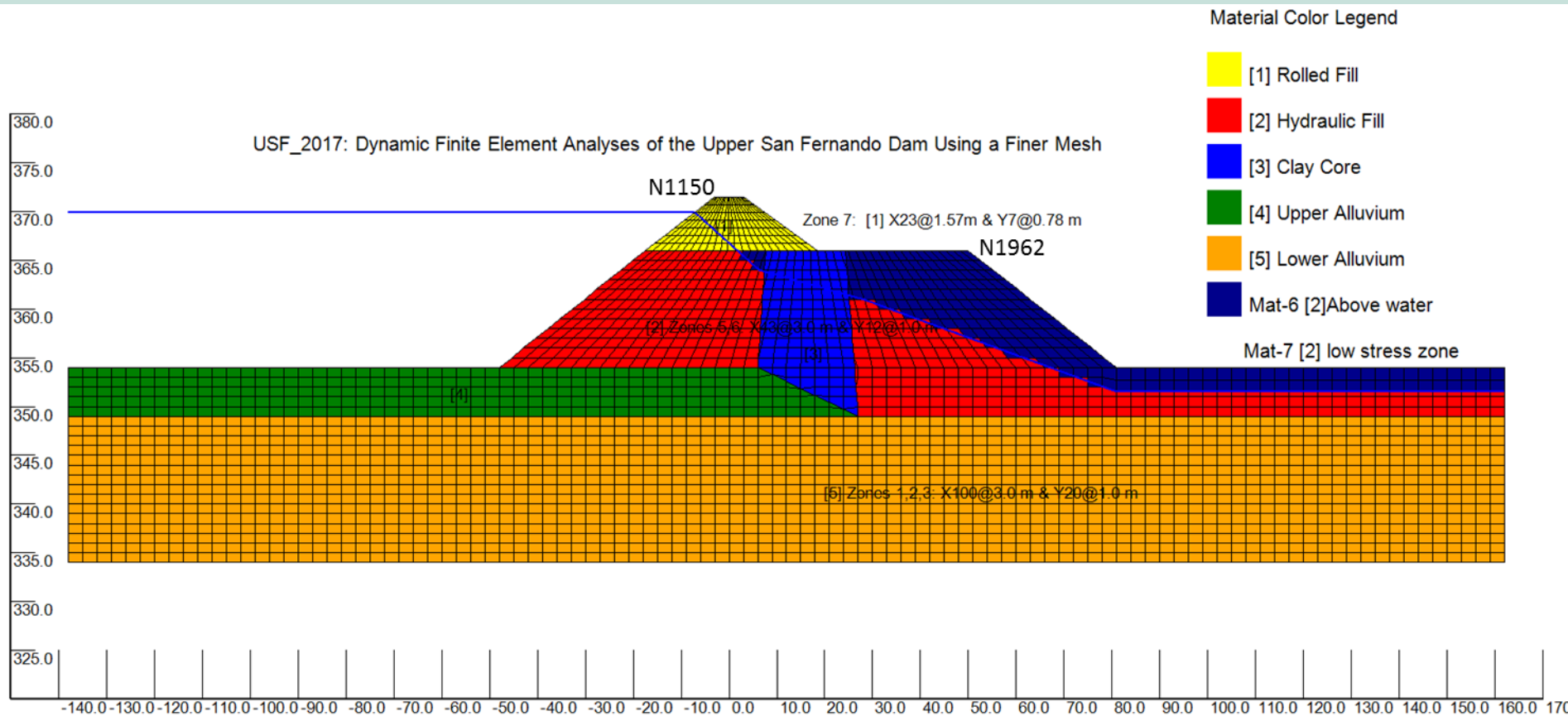


**Table 1. Soil stiffness and strength parameters of the Upper San Fernando Dam (Seed et al. 1973).**

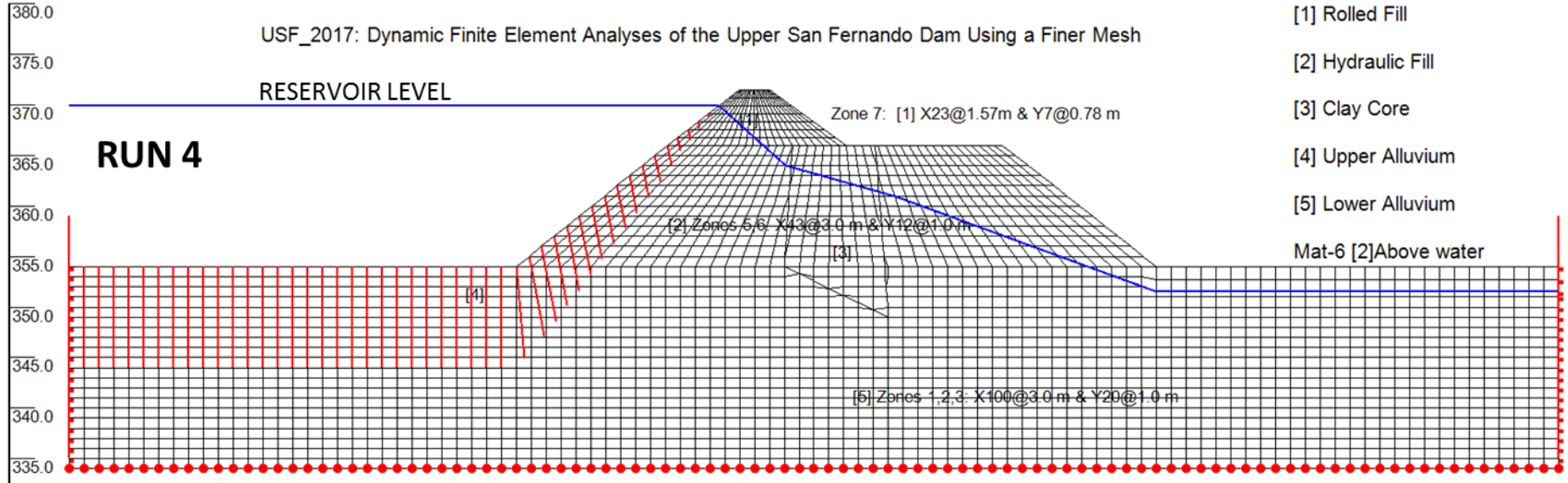
Soil unit	Soil material	Unit weight (kN/m <sup>3</sup> )	Strength parameters		Stiffness parameters*		
			$c'$ (kPa)	$\phi'$ (°)	$K_{2max}$	$K_g$	$K_b$
1	Rolled fill	22.0	124.5	25	52	1128	2821
2	Hydraulic fill	19.2	0	37	30	651	1630
3	Clay core	19.2	0	37	— <sup>†</sup>	651	1630
4	Upper alluvium	20.3	0	37	40	868	2170
5	Lower alluvium	20.3	0	37	110	2387	6000

\*Modulus exponents ( $m = n = 0.5$ ) were used for all soil units.

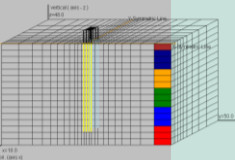
- **4.1 Case History Study by Finite Element Approach Analysis Of Upper San Fernando Dam Under The 1971 San Fernando Earthquake**
- [2] Model creation: Assign soil unit or material zones



- **4.1 Case History Study by Finite Element Approach Analysis Of Upper San Fernando Dam Under The 1971 San Fernando Earthquake**
- [3] Define soil parameters, Adjust D/S layer thickness, Set RUNs (layers, water tables, etc.), boundary, water loads



- [4] Run static analysis to obtain stresses with the existing dam  
Input file: *USF\_4\_FINAL.stat*

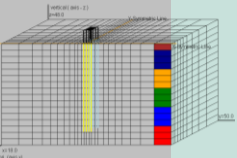


- **4.1 Case History Study by Finite Element Approach Analysis Of Upper San Fernando Dam Under The 1971 San Fernando Earthquake**
- [5] Conduct the dynamic analysis:
  - setup the dynamic run in 5 minutes
  - Setup moduli and pwp parameters for dynamic
  - Create a text file for input ground motion
  - Save and run to completion in 15 minutes

**Table 4.** Pore-water pressure parameters and residual strengths used in Seed et al. (1976) pore-water pressure model.

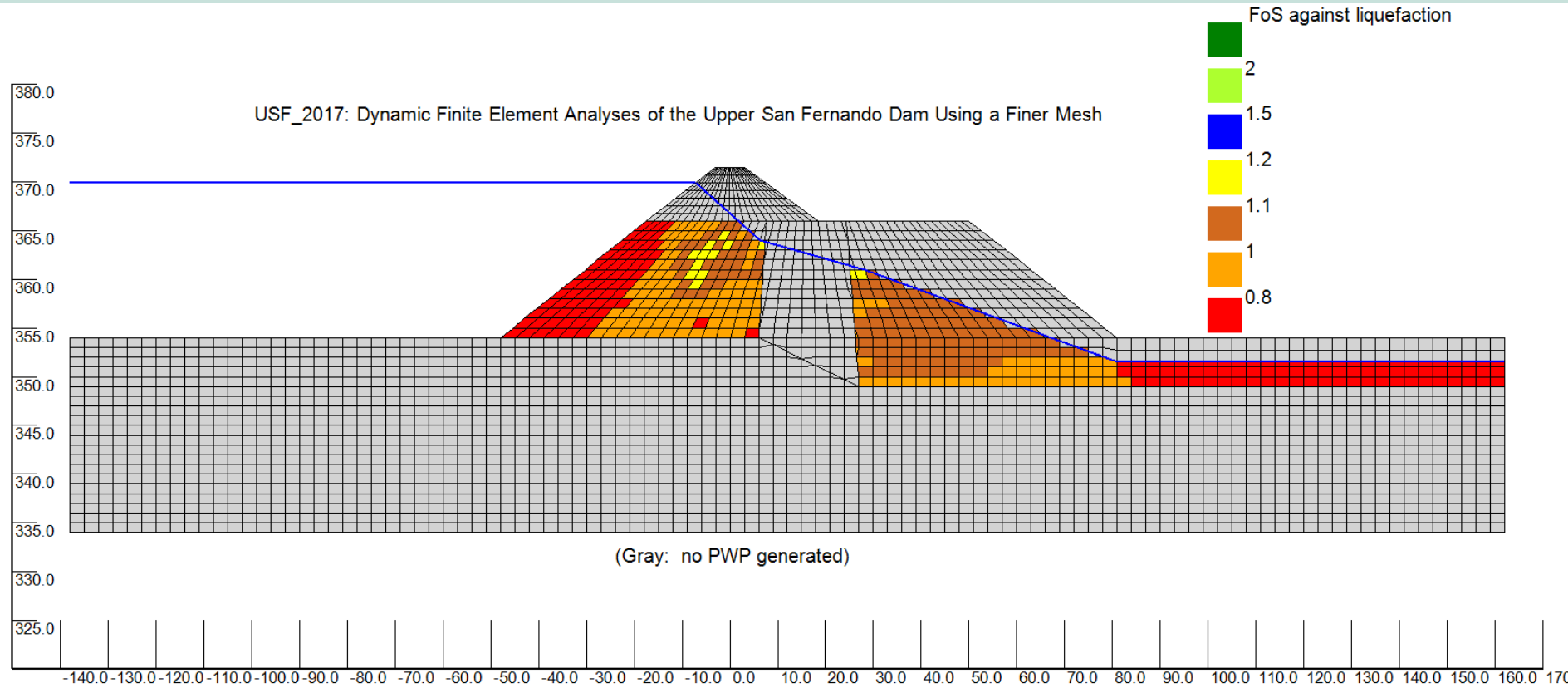
Material No.	Soil description	Equivalent $(N_1)_{60}$	CRR	$\alpha$	$\theta$	Residual strength (kPa)*	$K_c$ LIQ
2a	Upstream hydraulic fill	14	0.154	3.0	0.1	23.0 (480)	400
2b	Downstream hydraulic fill	14	0.154	3.0	0.1	23.0 (480)	400
2c	Hydraulic fill in the downstream free field	14	0.154	3.0	0.1	14.4 (300)	400

\* Pounds per square feet in parentheses.



- **4.2 Case History Study – Results Shown**
- [1] Factor of Safety Against Liquefaction using Seed's PWP model

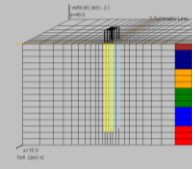
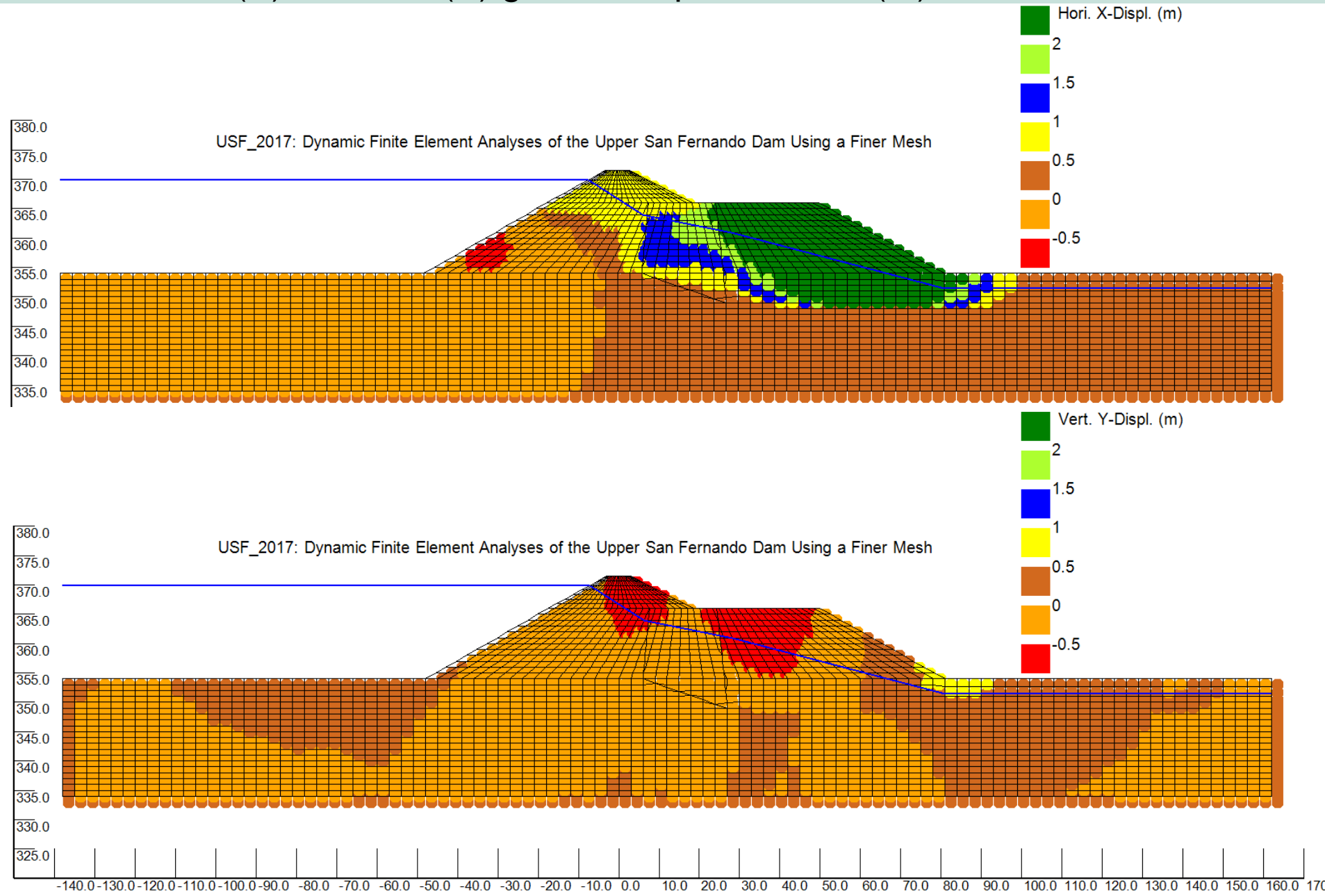
$FOS_{liq} < 1.0$  is considered liquefied in earthquake



# Dynamic effective stress analysis using the finite element approach by Dr. G. Wu

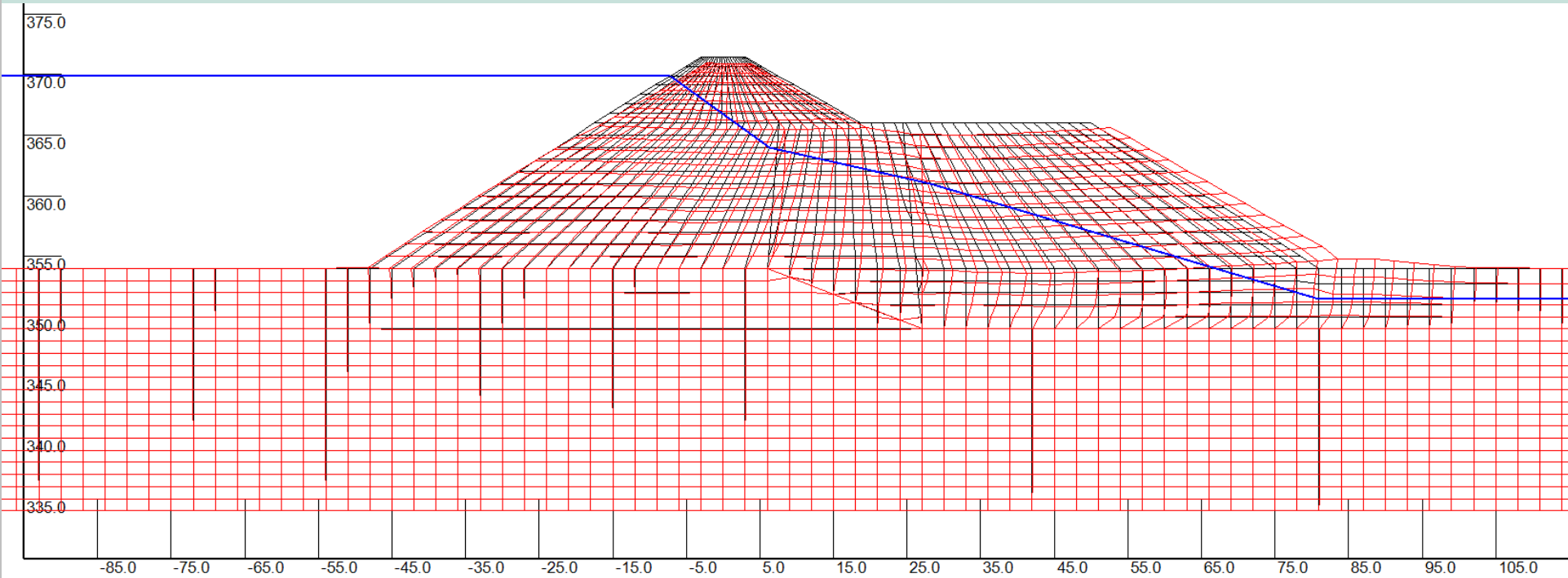
## 5. Case History - USF

- **4.2 Case History Study – Results Shown**
- Horizontal (X) and Vert (Y) ground displacements (m)



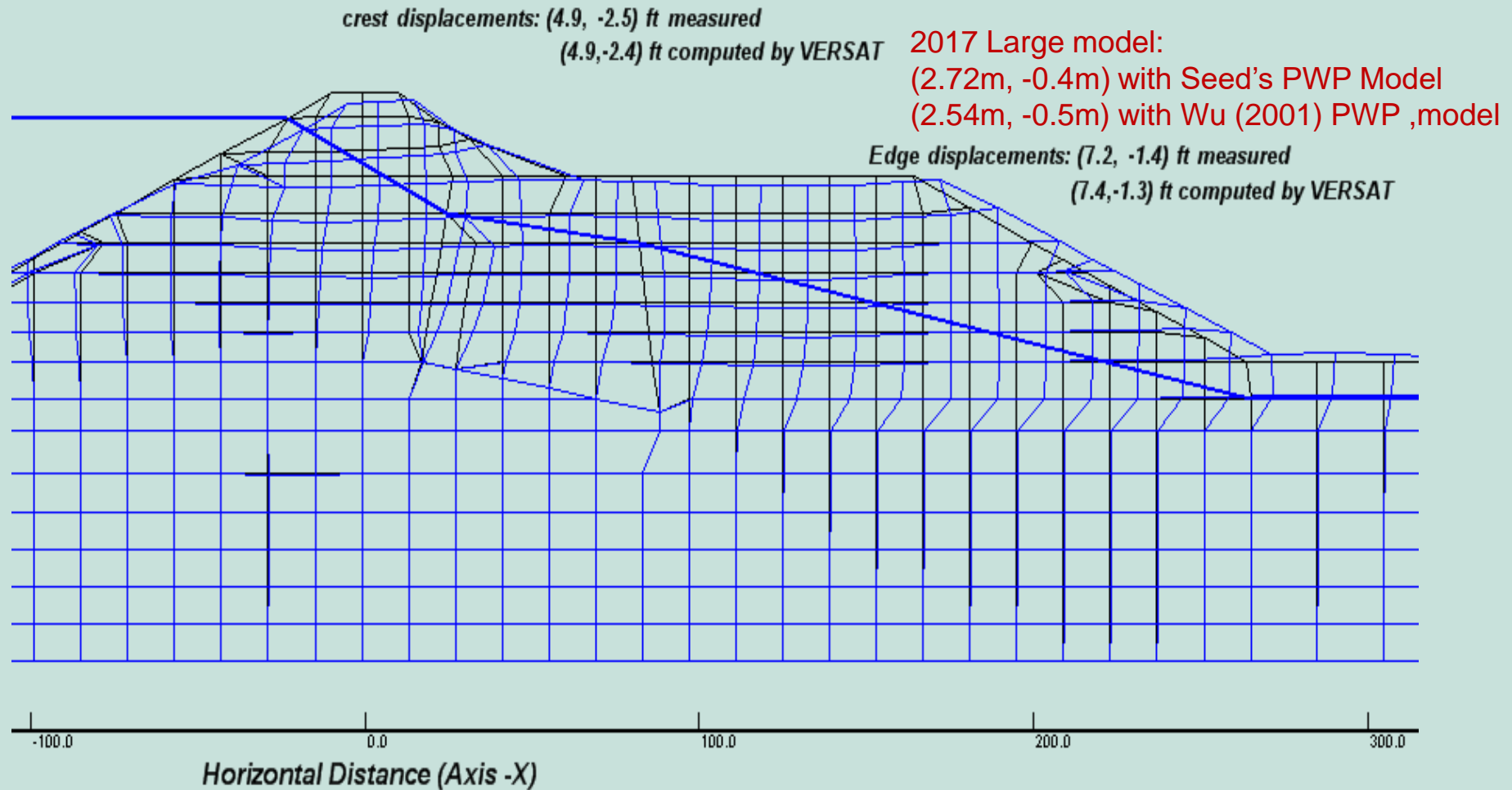
- **4.2 Case History Study – Results Shown**  
2017 large model with 2835 Nodes and 2704 Elements

Deformed Ground (RED) on original ground (black) with Seed's PWP model



Note: Feb. 2017 Computed displacements at Node points:  
N1150 (0.77 m, -0.52 m); N1962(2.72m, -0.40m) with Seed's PWP Model;  
N1150 (0.42 m, -0.44 m); N1962(2.54m, -0.50m) using Wu(2001) PWP Model:

- 4.3 Results from Wu (2001) Small Model:**  
678 nodes and 625 elements used in Wu (2001) model    **The dynamic analysis results are robust, consistent between 2001 small and 2017 large model.**



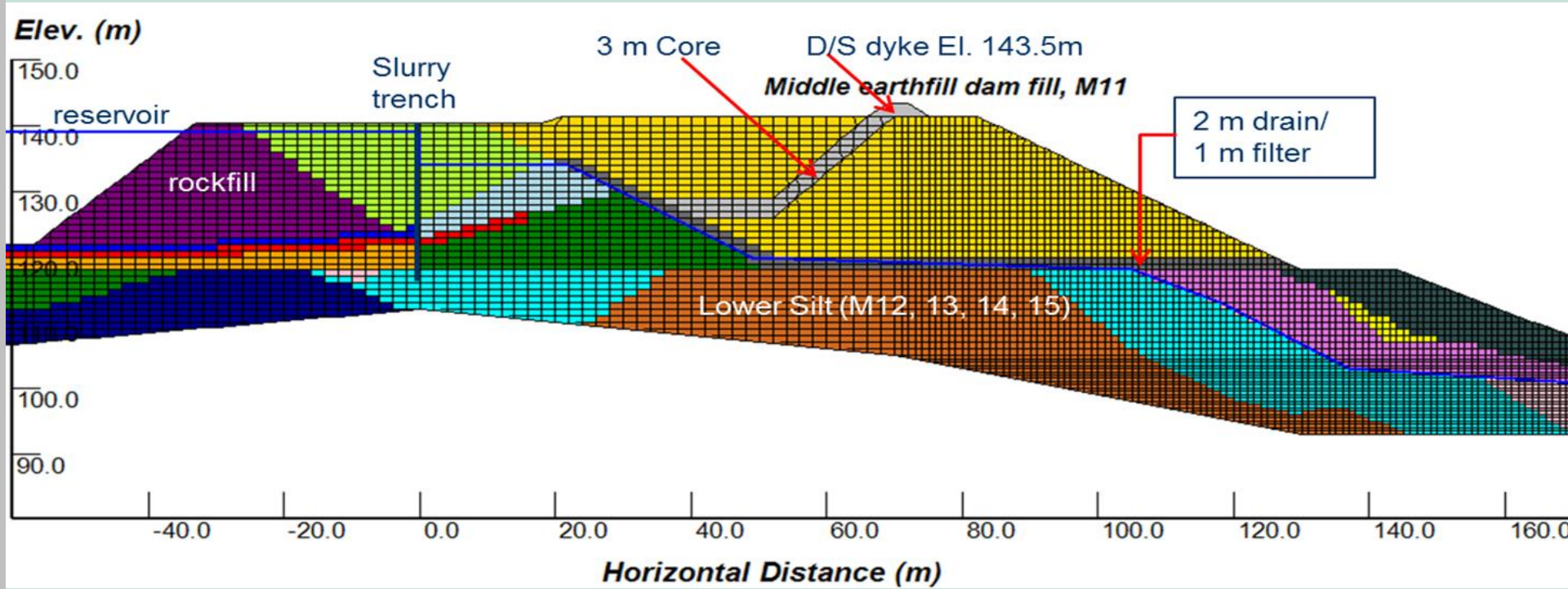
Wu, G. 2001. Earthquake induced deformation analyses of the Upper San Fernando dam under the 1971 San Fernando earthquake. Canadian Geotechnical Journal, 38: 1-15.

[Download Now](#)

# Dynamic effective stress analysis using the finite element approach by Dr. G. Wu

## 6. Other Case Studies

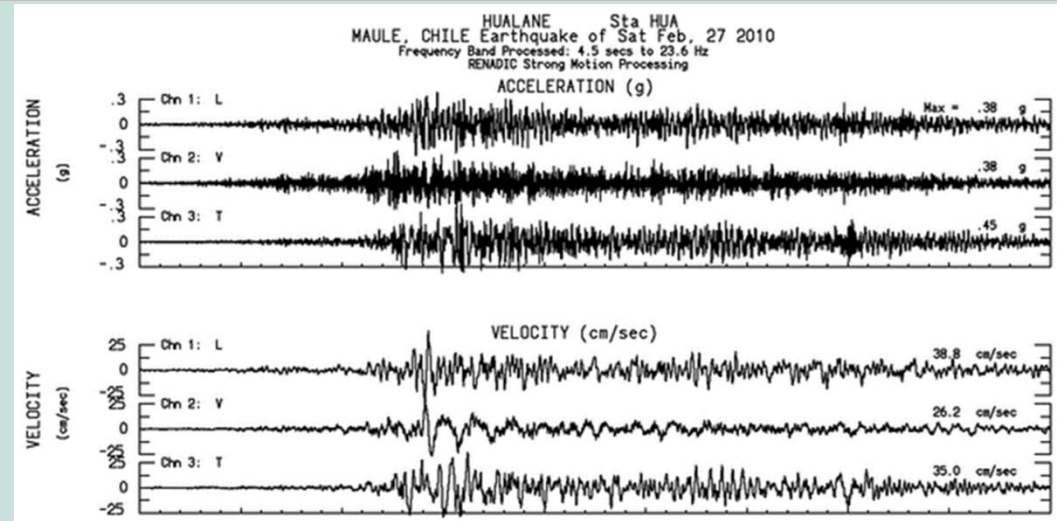
John Hart Middle Earthfill Dam (2013 Analysis): using “**VERSAT-SILT**” Model for the Silt



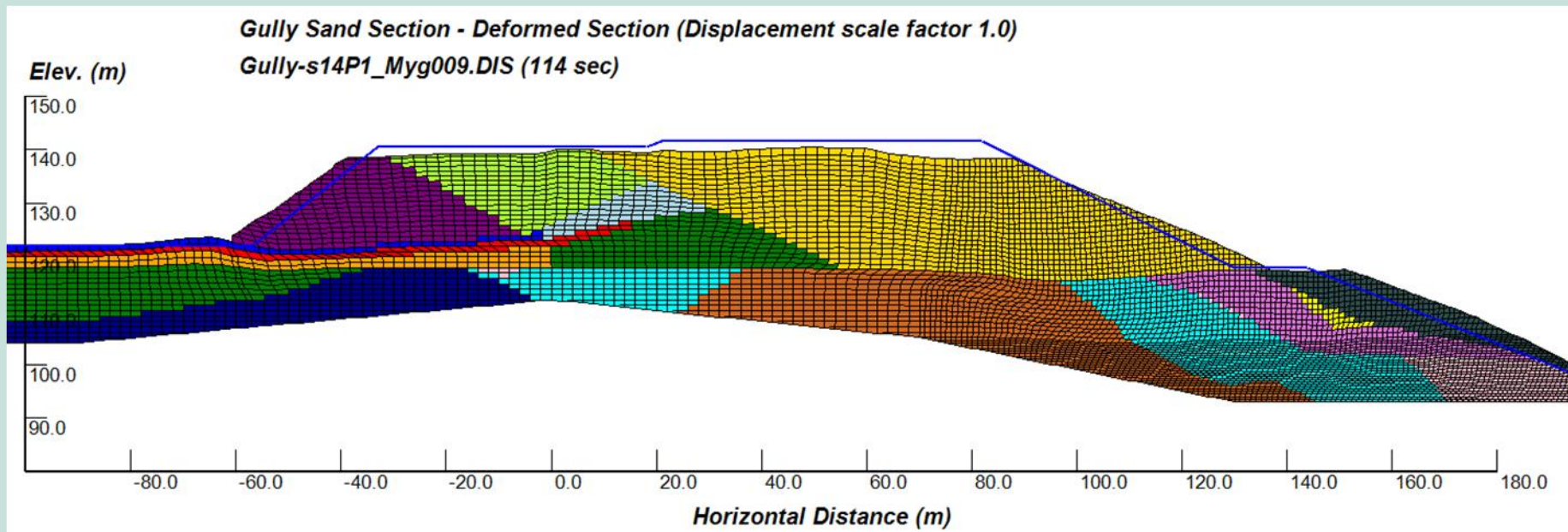
# Dynamic effective stress analysis using the finite element approach by Dr. G. Wu

## 6. Other Case Studies

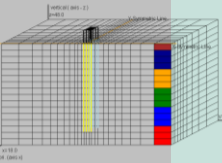
**2013 Dynamic Analyses:**  
Input motions =>



Computed ground deformation:



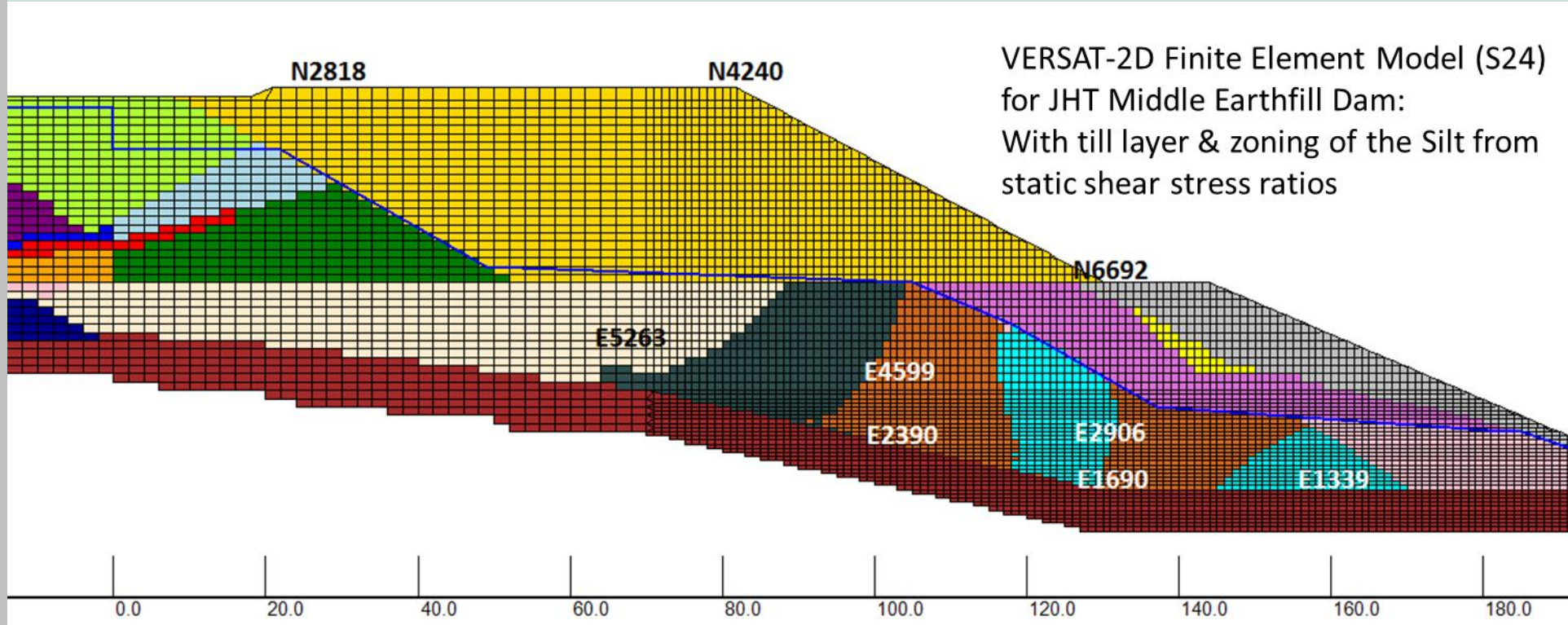
Finn W.D.Liam and Wu, Guoxi, 2013. Dynamic Analyses of an Earthfill Dam on Over-Consolidated Silt with Cyclic Strain Softening. Keynote Lecture, Seventh International Conference on Case Histories in Geotechnical Engineering, Chicago, US, April 29 - May 4. [Download Now](#)



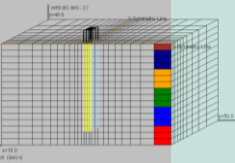
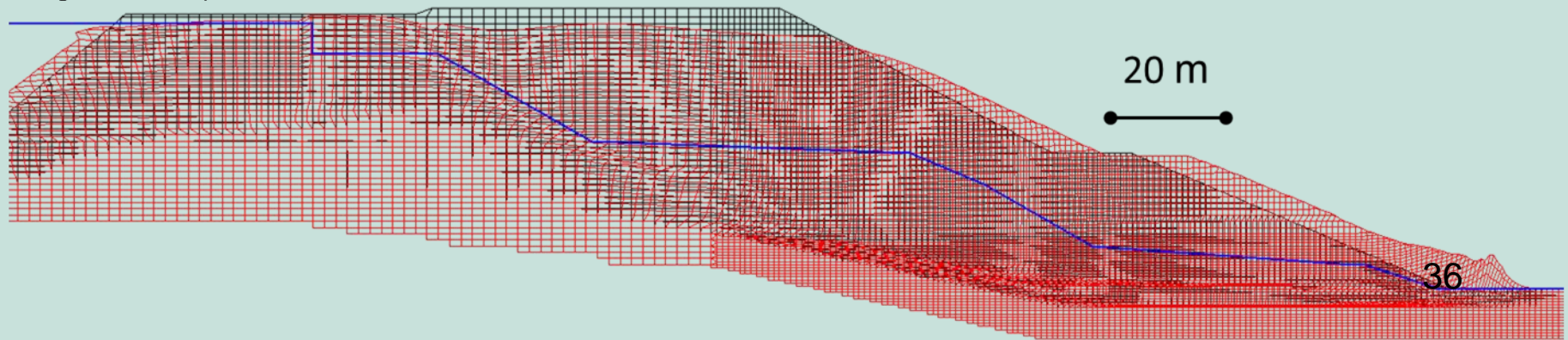
# Dynamic effective stress analysis using the finite element approach by Dr. G. Wu

## 6. Other Case Studies

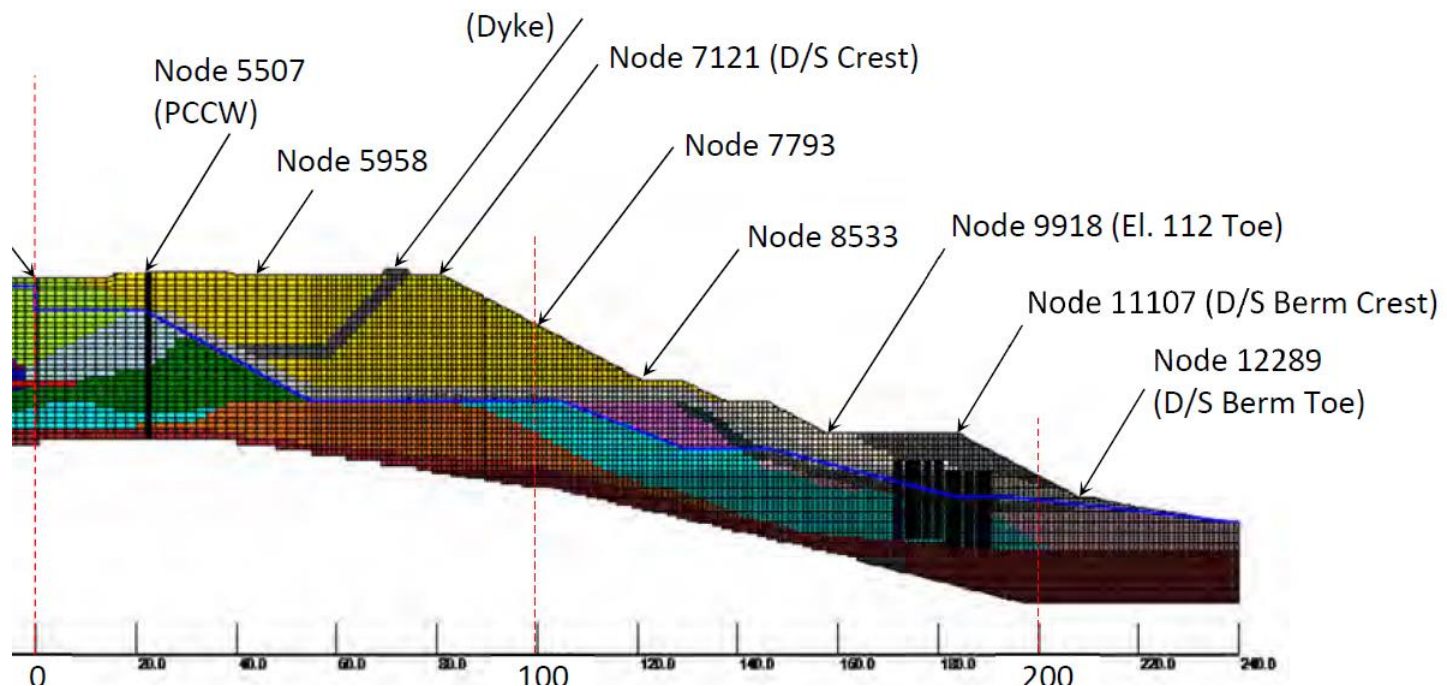
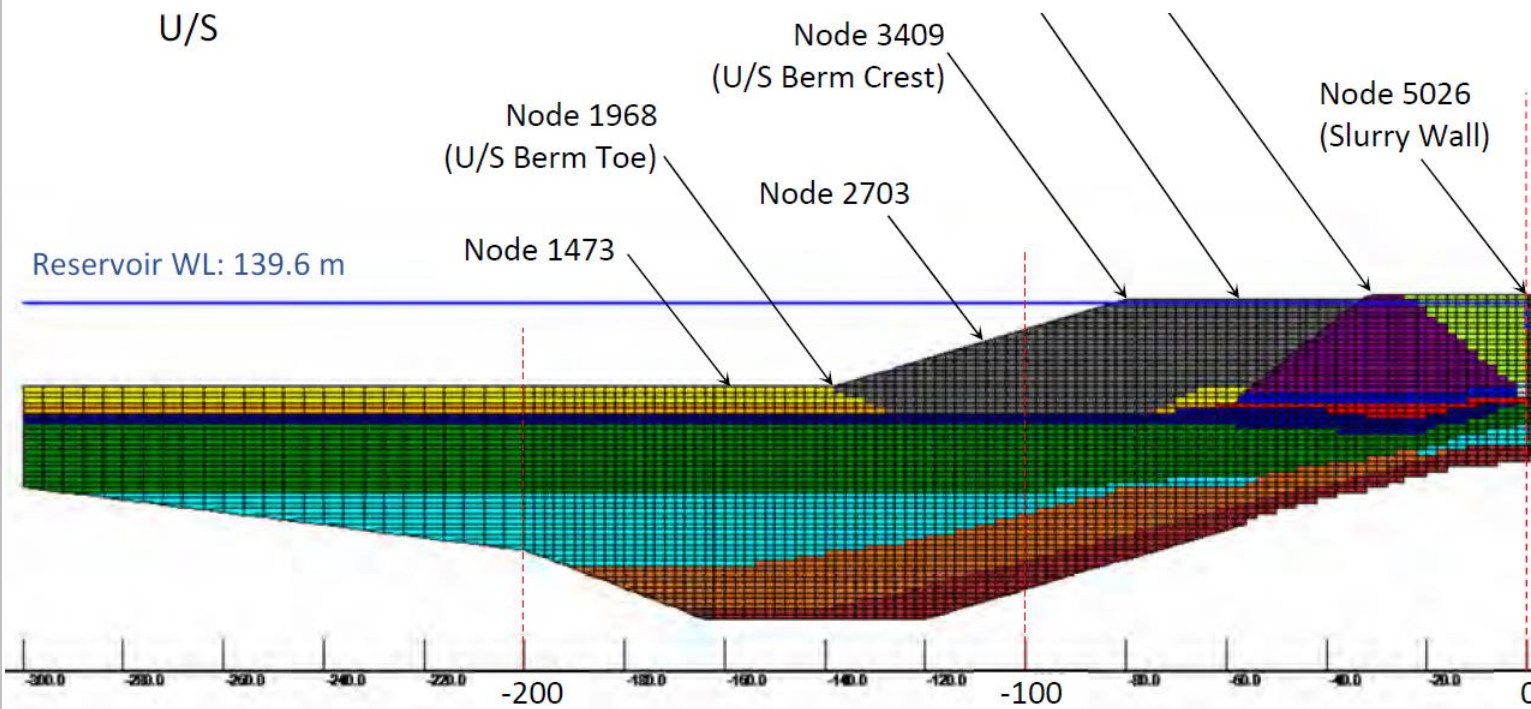
2016 Dynamic Analyses: *For academic research only (not for design)*



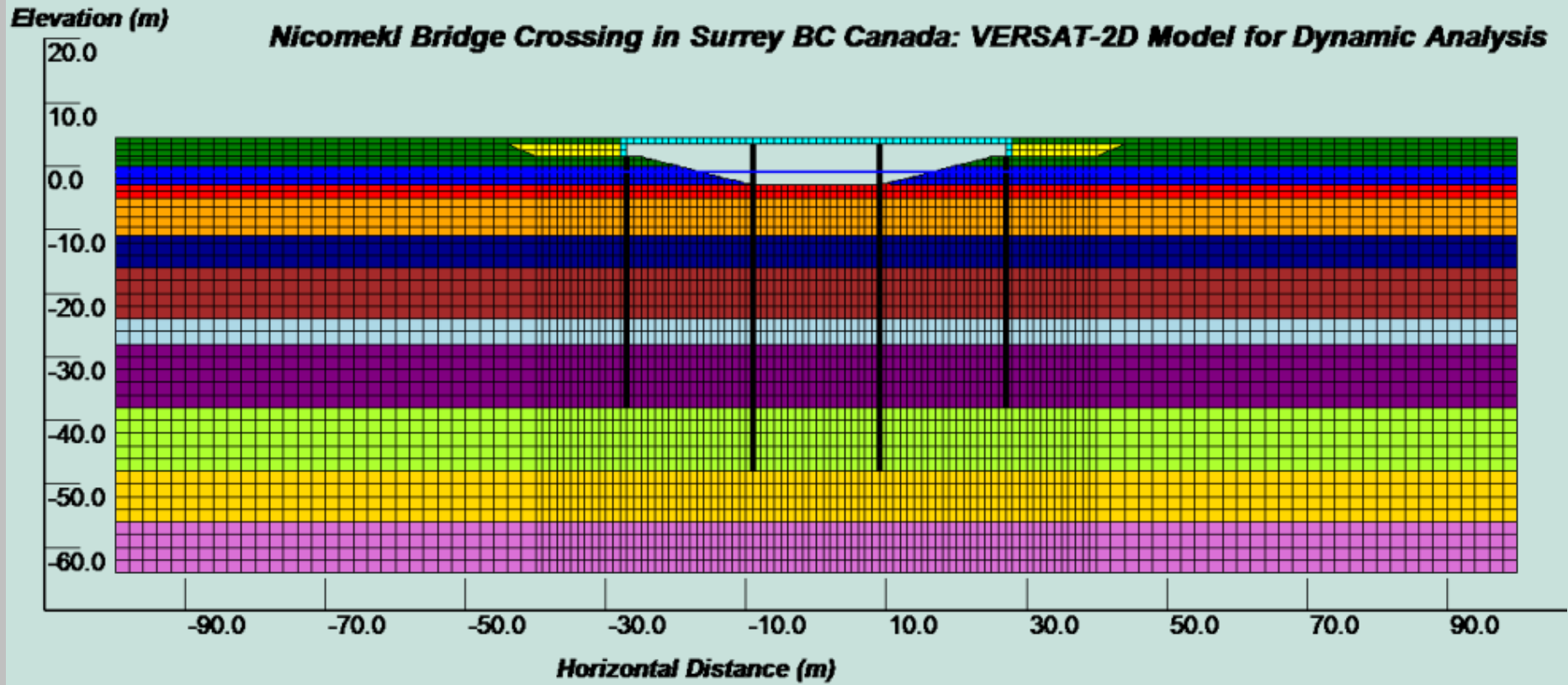
Gully\_s24RC\_P1Hual  
(assuming remolded shear strengths in Silt)



**VERSAT 2D  
Model with  
13417  
Elements**

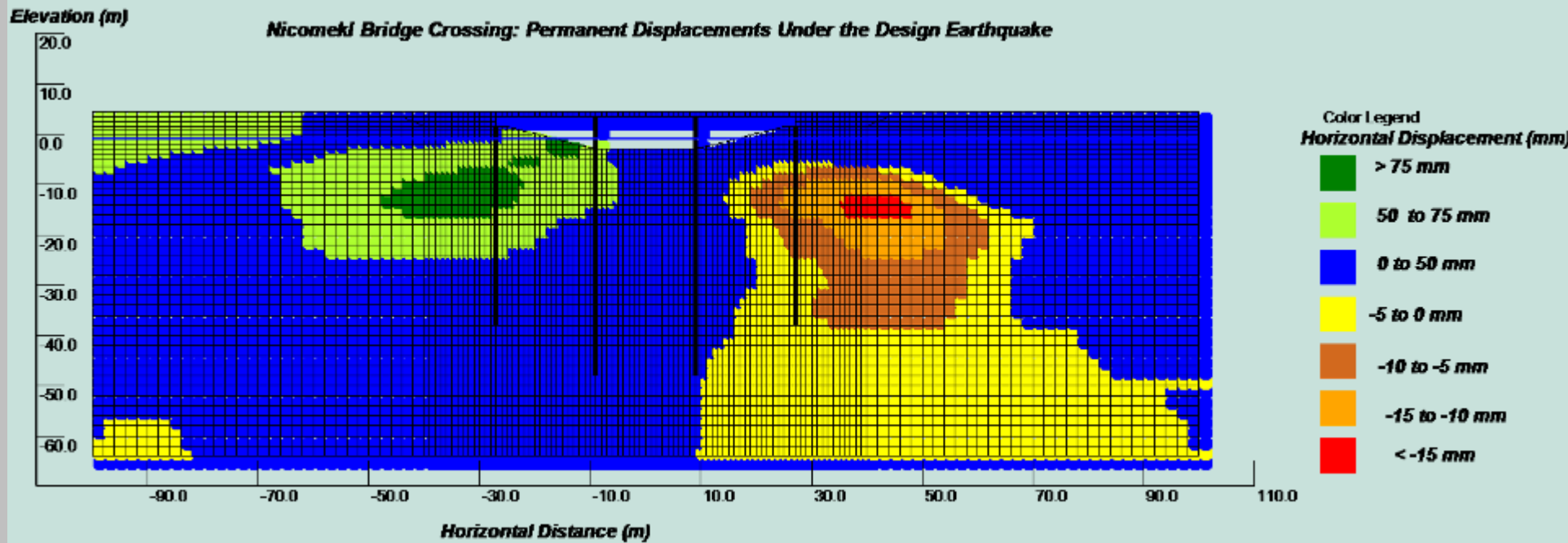


# New Serpentine River Bridge

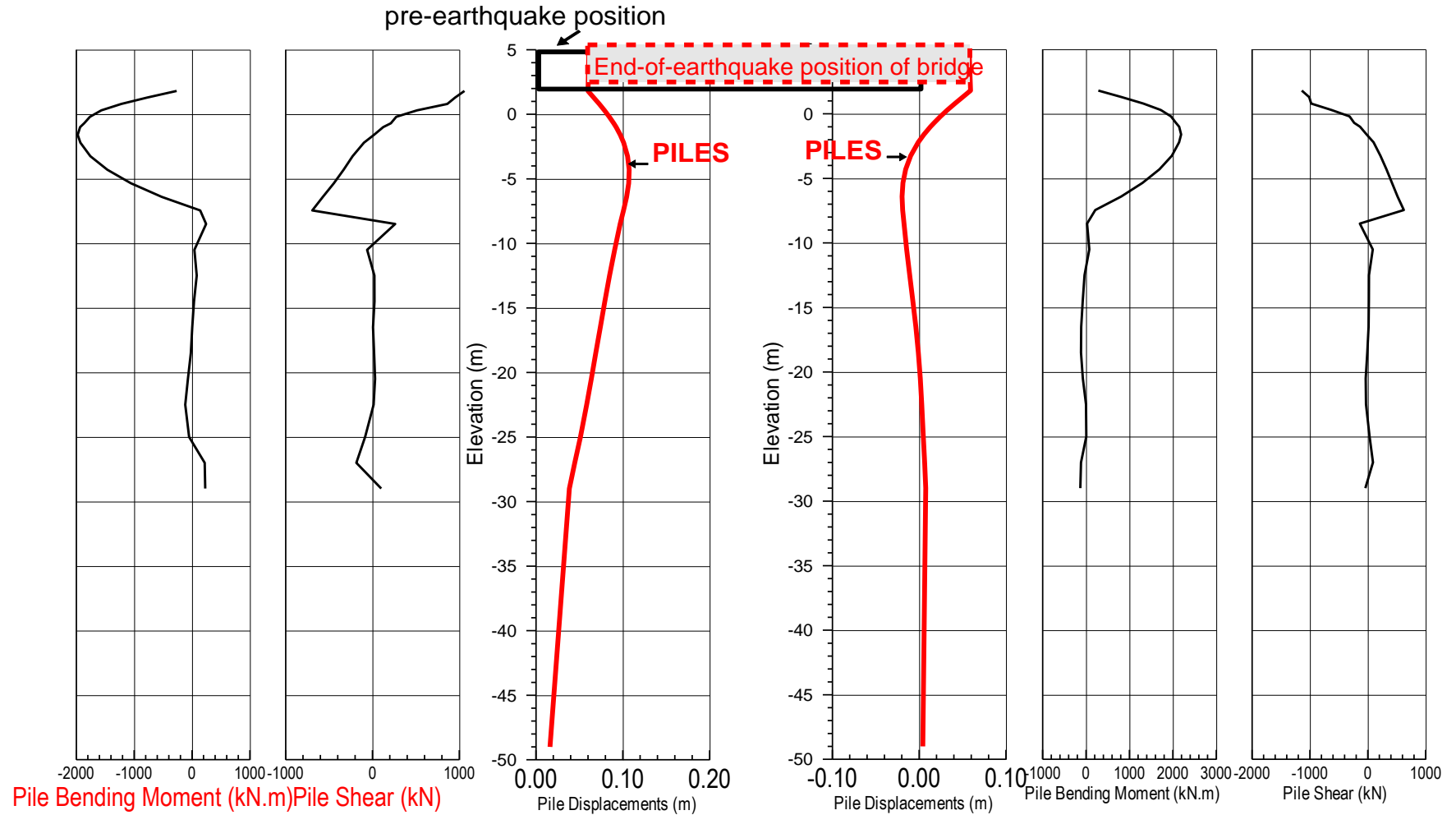


- Single Span Bridge on Soft Soils (24 m long, 14 m wide)
- 4716 nodes, 4572 elements, including bridge deck and abutment walls (Source: 2006 59<sup>th</sup> Can. Geot. Conference)

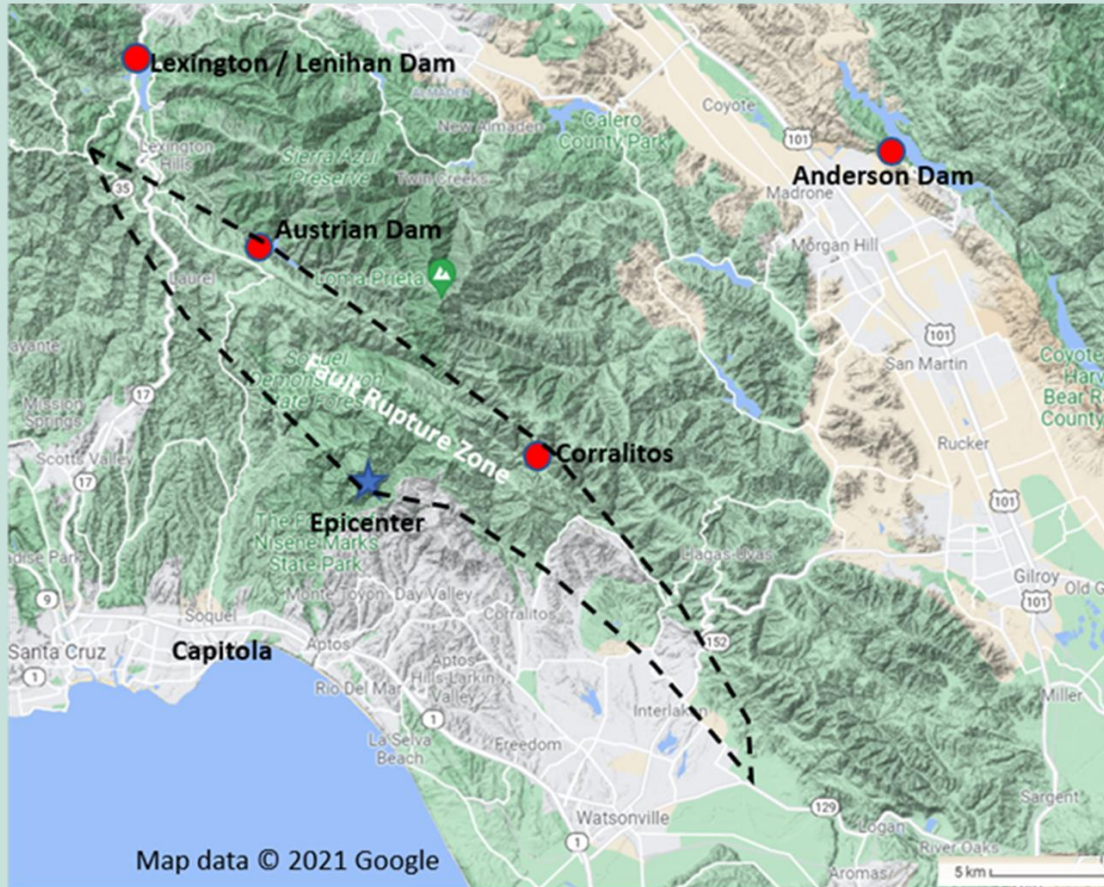
- End-of-earthquake horizontal displacement contours



- End-of-earthquake displacements of piles and bridge

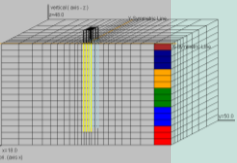


- **Lenihan and Austrian Dams** under the 1989 Loma Prieta Earthquake

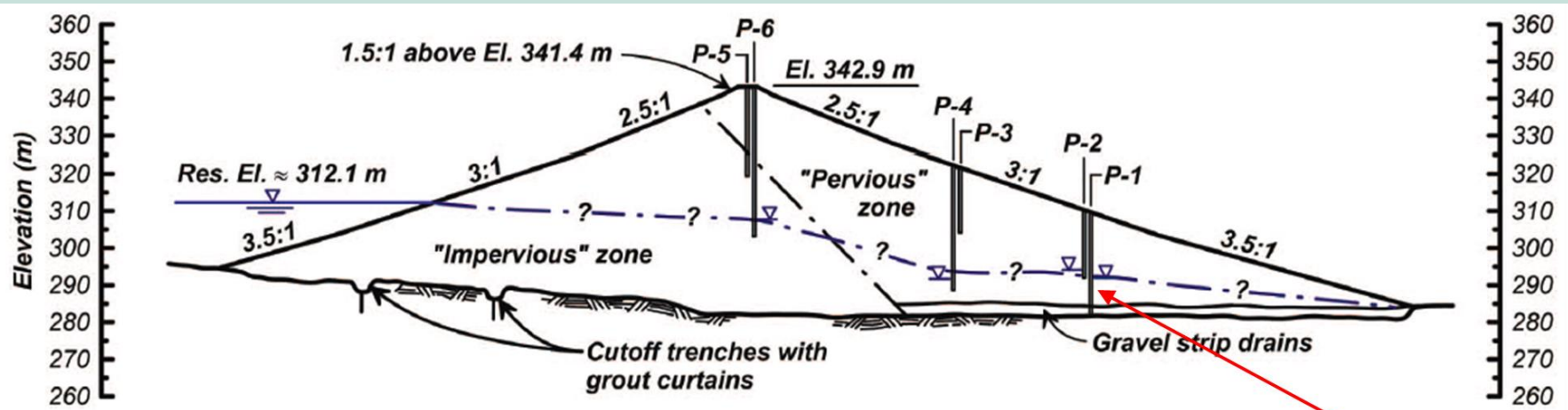


1. The 1989 October 17 Loma Prieta earthquake fault rupture zone (Mw 6.93)
2. Ground motion recording stations (the Lexington station and the Corralitos station) and
3. Austrian Dam in California with a horizontal PGA 0.55-0.6 g (Harder et al. 1998)

Wu, Guoxi. 2023. Case History Studies of Lenihan and Austrian Dams under the 1989 Loma Prieta Earthquake. In Proceeding Geo-congress 2023 in Los Angeles, USA, March.



• **Lenihan and Austrian Dams** under the 1989 Loma Prieta Earthquake

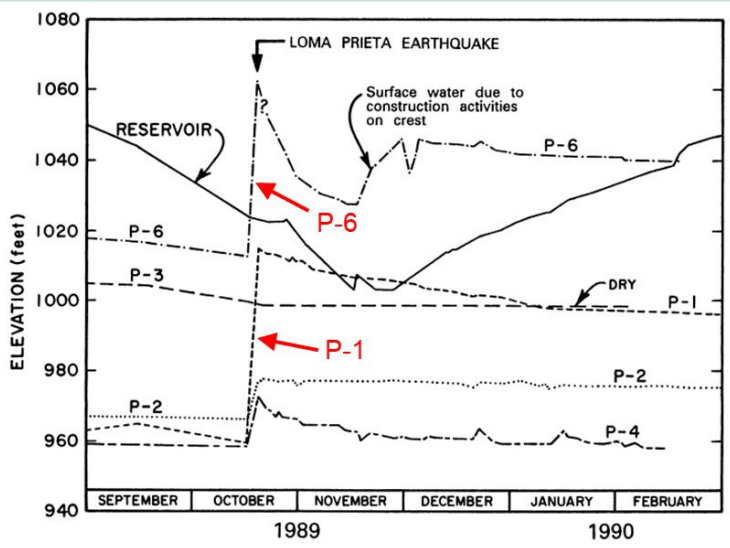


Shear deformations

MAXIMUM CROSS SECTION

**Damages by the earthquake:**

- Rise of PWP in P-1, P-6, P-2, and P-3. PWP heads increased 15.2 m in P-6 and 16.8 m in P-1 two days after the EQ
- Standpipe in piezometer P-1 significantly deformed at El. 291-293 m), suggesting earthquake induced internal movements due to lateral spreading (Harder et al. 1998)

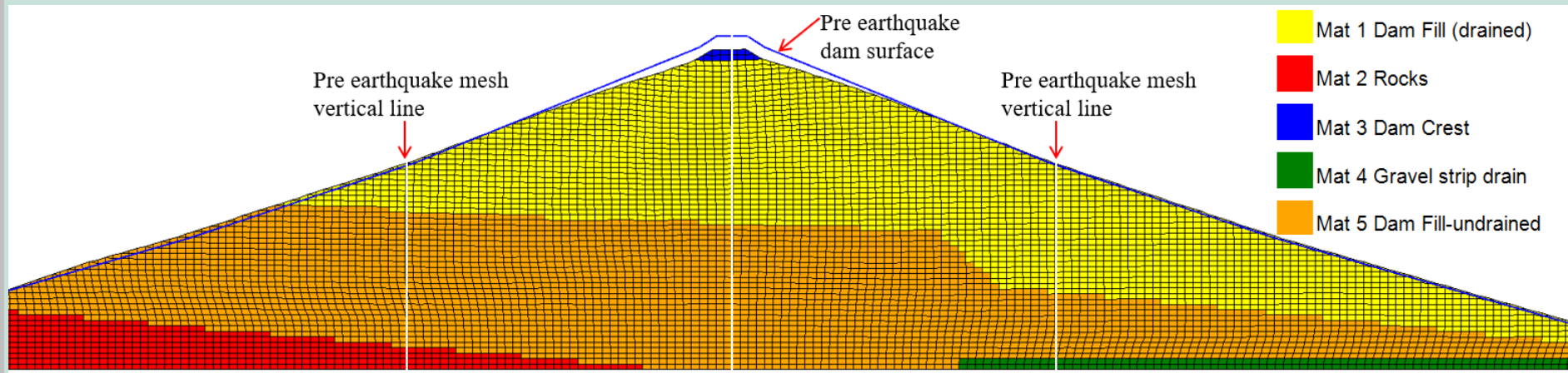
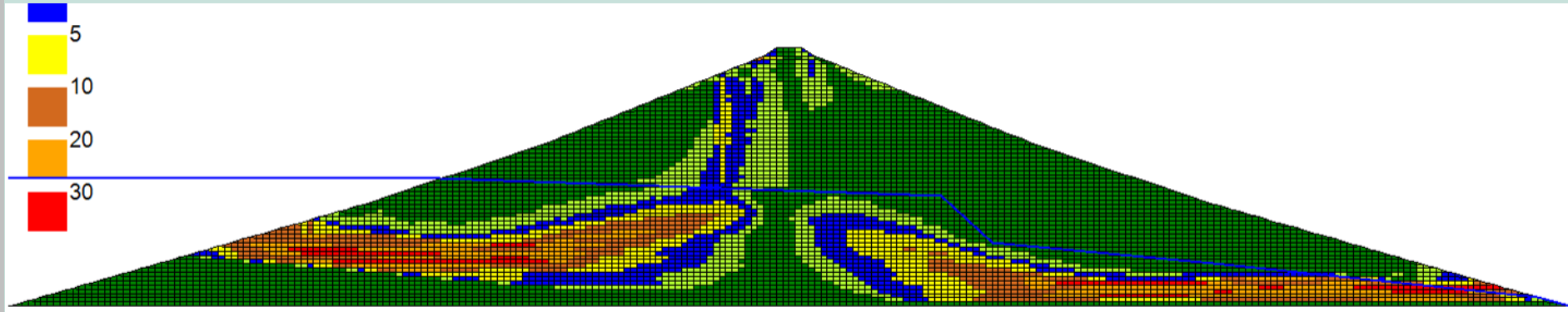


# Dynamic effective stress analysis using the finite element approach by Dr. G. Wu

## 6. Other Case Studies

2017 Lecture for CIVL 581 at University of BC by Dr. Guoxi Wu of BC Hydro / Wutec Geot.

Wutec Geotechnical International

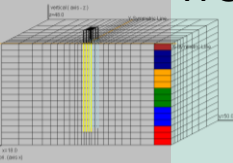


WGI (Wutec Geotechnical International). 2022. **Finite Element Dynamic Analyses of Austrian Dam.**

Engineering Report No. WGI-220224 (100 pages) <http://wutecgeo.com/publication.aspx>

WGI (Wutec Geotechnical International). 2022. **Case Study of Lenihan Dam under the 1989 Loma Prieta**

**Earthquake.** Engineering Report No. WGI-220301 (100 pages) <http://wutecgeo.com/publication.aspx>



# Dynamic effective stress analysis using the finite element approach by Dr. G. Wu

7. End



## Contact:

G. Wu, Ph.D., P. Eng.  
Wutec Geotechnical International  
406 – 615 Hamilton Street  
New Westminster, Metro Vancouver  
B.C., Canada, V3M 7A7

Email: [gwu@wutecgeo.com](mailto:gwu@wutecgeo.com)

Website: <http://www.wutecgeo.com>

THANK YOU !!  
谢谢 !!

